Final Report 2001-12

Research

Fine Particle (Nanoparticle) Emissions on Minnesota Highways

Technical Report Documentation Page

1. Report No.	2.	3. Recipients Accession No.
MN/RC – 2001-12		

4. Title and Subtitle	5. Report Date
Fine Particle (Nanoparticle) Emissions On Minnesota Highways	May 2001
	6.

7. Author(s)	8. Performing Organization Report No.
David B. Kittelson, Winthrop F. Watts, Jr., Jason P. Johnson	

9. Performing Organization Name and Address	10. Project/Task/Work Unit No.
Department of Mechanical Engineering University of Minnesota 111 Church St. SE Minneapolis, MN 55455	11. Contract (C) or Grant (G) No. c) 74708 wo) 120

12. Sponsoring Organization Name and Address	13. Type of Report and Period Covered
Minnesota Department of Transportation 395 John Ireland Boulevard Mail Stop 330 St. Paul, Minnesota 55155	Final Report 1999-2001
	14. Sponsoring Agency Code

15. Supplementary Notes

16. Abstract (Limit: 200 words)

This study examined the physical characteristics of combustion aerosols found on Minnesota highways. It emphasized the characterization of nanoparticles (less than 50 nm) with the goal of providing real-world data for the development of engine laboratory test methods.

On-road particulate matter emissions ranged between 10^4 to 10^6 particles/cm^3 with the majority of the particles by number being less than 50 nm in diameter. High-speed traffic produced high nanoparticle number concentrations and diesel traffic further increased number concentrations. At high vehicular speeds, particulate matter emissions increase because of higher engine load and fuel consumption. Measurements made at speeds less than 20 mph showed lower number but higher volume concentrations and larger particles.

Measurements made 10-30 m from the highway in residential areas approached on-road concentrations with similar size distributions and high concentrations of nanoparticles. Lower concentrations and larger particles were observed in residential areas 500 to 700 m from the highway.

Fuel specific and particle/mi emission rates were estimated from data collected on two different days. The particle/mi emissions were about an order of magnitude greater than published figures but mass emission rates compared well with published values. However, colder temperatures, different dilution and sampling conditions and different instrumentation could explain our increased estimates.

17. Document Analysis/Descriptors	18. Availability Statement
Combustion aerosol Nanoparticle measurement Transportation aerosol measurement	No restrictions. Document available from: National Technical Information Services, Springfield, Virginia 22161

19. Security Class (this report)	20. Security Class (this page)	21. No. of Pages	22. Price
Unclassified	Unclassified	87	

FINE PARTICLE (NANOPARTICLE) EMISSIONS ON MINNESOTA HIGHWAYS

Final Report

Prepared by

David B. Kittelson, Ph.D.,
Winthrop F. Watts, Jr., Ph.D.
And
Jason P. Johnson

University of Minnesota
Department of Mechanical Engineering
Minneapolis, MN 55455

May 2001

Published by:

Minnesota Department of Transportation
Office of Research & Strategic Services
Mail Stop 330
395 John Ireland Boulevard
St. Paul, MN 55155

ACKNOWLEDGEMENTS

The researchers would like to thank the Minnesota Department of Transportation for funding this research, through the University of Minnesota Center for Transportation Studies, and would also like to thank Bill Bunde and Marilyn Jordahl-Larson of Mn/DOT for serving as members of the Technical Advisory Panel and for providing oversight and assistance through the entire project period. We would like to thank the Coordinating Research Council (CRC) and the sponsors of the CRC E-43 project for the funding that allowed the University's Mobile Emissions Laboratory (MEL) to be built and instrumented. The E-43 sponsors include the Department of Energy National Renewable Energy Laboratory, the Engine Manufacturers Association, the Southcoast Air Quality Management District, the California Air Resources Board, the Cummins Engine Company Inc., Caterpillar Inc. and the National Institute of Occupational Safety and Health. We would like to extend a special thank you to the Volvo Truck Corporation for providing the tractor platform for the MEL. We would like to thank Mr. Jack Herndon, Jay Johnson and the rest of the crew at the Minnesota Department of Transportation's MnRoad test facility for their assistance in getting the MEL up and running. We thank Mr. Dwane Paulsen for designing, fabricating and evaluating the leaky filter dilutor used in the project. Lastly, we want to thank Mr. Marcus Drayton, Mr. Richard Beaudette and Ms. Erin Ische for their assistance in collecting and analyzing data. The assistance of these organizations and people made this project possible.

TABLE OF CONTENTS

LIST OF TABLES

LIST OF FIGURES

LIST OF ACRONYMS USED IN THIS REPORT

CO – Carbon monoxide

CO_2 – Carbon dioxide

CPC – Condensation particle counter

CRC – Coordinating Research Council

DC – Diffusion charger

DPM – Diesel particulate matter

EC – Elemental carbon

ELPI – Electrical low pressure impactor

EPA – Environmental Protection Agency

HEI – Health Effects Institute

MEL – Mobile emission laboratory

MTU – Michigan Technological Institute

NDIR – Non-dispersive infrared

NO_x – Oxides of nitrogen

OC – Organic carbon

PAS – Photoelectric aerosol sensor

PM – Particulate matter

PM2.5 – Particulate matter, < 2.5 μm in size

PM10 – Particulate matter < 10 μm in size

OC – Organic carbon

SI – Spark ignition

SMPS – Scanning mobility particle sizer

SOF – Soluble organic fraction

TC – Total carbon

UMN – University of Minnesota

EXECUTIVE SUMMARY

The objective of this project was to determine the physical characteristics of combustion aerosols found on Minnesota highways with major emphasis on characterizing particles < 50 nm in size (nanoparticles). Nanoparticles are of interest because it is important to develop engine test methods for the laboratory that reflect real-world emission characteristics. Initially sampling was to occur primarily at metered and non-metered on-off ramps but this was changed to accommodate the scheduled use of the University's Mobile Emissions Laboratory (MEL) on other projects. Rather than focusing on collecting data at ramps, data were collected on-road under varying traffic conditions and in residential areas different distances from the highway. When sampling in residential areas, data were collected upwind and downwind from the highway to determine the impact of highway traffic on residential air quality. Specifically, changes in aerosol concentration and size distribution over time and distance were observed. On-road aerosol concentrations and size distributions were obtained. These data were combined with gaseous emissions data to estimate fuel specific emissions and particle emissions per mile.

Nearly all data were collected in November 2000. Ambient air temperature and relative humidity ranged between 1-13^{o} C and 40 and 60 %, respectively. These conditions limit the study if the results are to be used to reflect particle number concentrations during summer months in Minnesota. Findings from studies conducted in our laboratory have shown that the formation of nanoparticles is greatly enhanced by cold temperatures, thus additional data must be collected during warmer periods to expand the comprehensiveness of the results.

The MEL was used throughout the study to collect data. The MEL is a self-contained mobile laboratory that is transported by a Volvo tractor. The lab is housed in a 6.1 m (20 ft) box

container with power supplied by two Onan generators. The lab may be off-loaded from the tractor and operated apart from it. Approximately $500,000 worth of instrumentation is housed in the MEL. The primary instruments used in the study to characterize on-road particulate matter emissions were the scanning mobility particle sizer (SMPS), condensation particle counter (CPC), and the electrical low-pressure impactor (ELPI). In addition, three gas analyzers, carbon monoxide (CO), carbon dioxide (CO_2,) and nitrogen oxides (NO_X), were used to characterize gaseous emissions on the highway.

On-road particulate matter emissions ranged between 10^4 to 10^6 particles/cm^3 with the majority of the particles by number being less than 50 nm in diameter. An association was observed between traffic speed and nanoparticle concentration: The higher the speed the greater the nanoparticle concentration and the smaller the particle size. This is a reasonable finding, because when the MEL was going 88 kmph (55 mph) the surrounding traffic was going 97 to 113 kmph (60 to 70 mph). At high vehicular speeds, particulate matter emissions increase because of higher engine load and fuel consumption. Passing diesel traffic was observed to further increase particle number concentrations. Measurements made in traffic jams with speeds < 20 mph showed lower concentrations and larger particles. Some of the particles observed at higher speeds might have resulted from transient release of particle-associated materials stored in exhaust systems during lower speed operation. Less variation was observed in particle volume compared to particle number size distributions. Particle volume is a surrogate measure of particle mass and is conserved while particle number is constantly changing due to adsorption, coagulation and other physical and chemical mechanisms.

Measurements made 10-30 m (33-98 ft) from the highway in residential areas where

highway airflow was not obstructed by barriers demonstrated that aerosol concentrations approached on-road concentrations. The size distribution in these areas was similar to on-road aerosol with high concentrations of very small (<20 nm) particles. Much lower concentrations and much larger particles were observed in residential areas located 500 to 700 m (0.3 to 0.4 mi) from the highway.

Fuel specific and particle/mi emission rates were estimated from data collected on two different days. The particle/mi emissions were about an order of magnitude greater than published figures based upon results from laboratory studies. However, colder temperatures, different dilution and sampling conditions and different instrumentation could explain our increased estimates. More data needs to be collected to improve and validate these estimates.

The data collected during this study represent a unique database that will provide information on on-road emissions under cold climatic conditions. Further studies need to be completed to provide a more complete set of data; especially under warmer climatic conditions.

CHAPTER 1
INTRODUCTION

Epidemiological and laboratory studies have linked environmental exposure to particles less than 2.5 μm in size to adverse health effects (1-8). These studies, however, have not established causal mechanisms nor have they focused on determining the physical characteristics of the aerosol to which people are exposed. The objective of this study is to determine the physical characteristics of transportation related nanoparticle aerosols on Minnesota roadways and to determine how these characteristics change over time, traffic conditions and engine type. This type of information is useful to industry, regulatory agencies, health professionals and others interested in knowing the characteristics of aerosols found on roadways under real-world traffic conditions. It is also useful to scientists working in engine test facilities who desire to develop test methods that produce results that reflect real-world emission characteristics. This report is divided into sections. Background information is provided to assist the reader in understanding the problem. This is followed by descriptions of the MEL and instrumentation, and the methods and approach used to collect data. Finally the results, discussion and summary are presented.

Objective

The objective of this study was to determine the physical characteristics of transportation related nanoparticle aerosols on Minnesota roadways and determine how these characteristics change over time, traffic conditions and engine type. Aerosol data were originally to be obtained using the University of Minnesota's Mobile Emissions Laboratory (MEL) parked near metered and non-metered on ramps and on highways under congested and uncongested conditions.

However, the study was modified to accommodate the demands of other projects requiring use of the MEL. Rather than focusing on collecting data at ramps, data were collected on-road under varying traffic conditions and in residential areas different distances from the highway. When sampling in residential areas, data were collected upwind and downwind from the highway to determine the impact of the highway on residential air quality and to determine the effects of aerosol aging on the plume aerosol concentration and size distribution. On-road size distributions and fuel specific emissions were obtained.

The MEL was built and instrumented using funds from other sponsors at no cost to the project. Figure 1 shows the MEL chasing a Cummins tractor down a rural Minnesota road. The MEL is unique in its capability to monitor transportation related aerosols and gases and to determine detailed physical characteristics of nanoparticles.

Background – Understanding the Problem

An aerosol size distribution can be characterized based upon particle mass, number, surface area or volume and a relationship exists between particle size and deposition in the respiratory system because deposition is a function of particle size. As aerodynamic particle size decreases below about 0.25 μm (250 nm) deposition increases in the deep region (alveolar region) of the lung. Figure 2 illustrates relationships between idealized combustion aerosol number and mass weighted size distributions (9) and the alveolar deposition curve (10-11). In this case the distribution typifies a diesel aerosol distribution. A spark-ignition (SI) size distribution is similar but less well defined. The mass median diameter of SI aerosol is typically smaller; the aerosol is composed of a higher proportion of organic carbon (OC) and less elemental carbon (EC).

Combustion aerosol follows a lognormal, trimodal size distribution, as illustrated in figure 2, with the concentration in any size range being proportional to the area under the corresponding curve in that range. Nuclei-mode particles range in diameter from 0.005 to 0.05 μm (5-50 nm). [A meter has 1 x 10^9 nanometers (nm) or 1 x 10^6 micrometers (μm)]. They consist of metallic compounds, EC and semi-volatile organic and sulfur compounds that form particles during exhaust dilution and cooling. For diesel aerosol, the nuclei mode typically contains 1-20 % of the particle mass and more than 90 % of the particle number. The accumulation mode ranges in size from roughly 0.05 to 0.5 μm (50-500 nm). Most of the mass, composed primarily of carbonaceous agglomerates and adsorbed materials, is found here. The coarse mode consists of particles larger than 1 μm and contains 5-20 % of the mass. These relatively large particles are formed by reentrainment of particulate matter, which has been deposited on cylinder, and exhaust system surfaces. Also shown in figure 2 are size range definitions for atmospheric particles: PM10 (diameter < 10 μm), fine particles (diameter < 2.5 μm), nanoparticles (diameter < 0.05 μm or < 50 nm), and ultrafine particles (diameter < 0.10 μm or < 100 nm).

Regulatory agencies such as the Environmental Protection Agency (EPA) have adopted air pollution regulations for particulate matter less than 2.5 μm in size (PM2.5) and increasingly stringent exhaust emission regulations that reduce the mass or particulate matter emitted from engines. However, other metrics beside mass may be important in characterizing the physical properties of aerosol important to health (12). These include the number and surface area of the particles.

Particulate matter (PM) emissions from internal combustion engines have traditionally been regulated solely on the basis of total particulate mass emissions; no reference is made either

to the size or the number concentration of the emitted particles. Modern engines emit much lower particle mass concentrations. Recent research suggests that for diesel engines the reduction in particle mass may be accompanied by an increase in the number of nanoparticles (13). Furthermore, as shown in this project and others (14) there is a correlation between local traffic patterns and ambient particle number concentration, while there is little correlation with ambient mass concentration. Recent measurements show that ambient number concentrations in busy urban areas can reach 4×10^6 particles/cm^3, even though ambient mass concentrations are well below regulated limits (15-16).

Understanding the fundamental science underlying particle formation and measurement is critical to research organizations such as universities, health and environmental organizations, and local and state governments. Sound science dictates that future environmental decisions be based an understanding of the causes and effects of pollution. Further, it is important that data collected in the engine test laboratory be representative of actual ambient conditions, so that future environmental decisions are based on data that are not compromised by possible artifacts resulting from laboratory conditions. Our findings will assist in the decision process by providing a basis for determining whether laboratory results are real or an artifact of laboratory sampling methods. This information is critical for regulators interested in limiting fine particle emissions. Further, data collected under varying traffic conditions will allow a quantitative determination of the environmental impact of traffic on the surrounding area.

A brief synopsis of studies that have measured and characterized particulate matter emissions from diesel and gasoline fueled engines is presented to assist in interpreting data collected during this project.

Spark Ignition Emissions

Modern SI engines have much lower particulate matter mass emission rates than diesel engines (17) but recent studies suggest that number-weighted nanoparticle emissions from SI engines may be very significant (18-22). Under high power (~120 km/hr road load or 75 mph), SI engines emit particle number concentrations that are comparable to those from diesel engines with a similar power rating. Under cold start and high power conditions the fuel to air ratio is not stoichiometric but is "rich". This causes much higher exhaust particle number concentrations compared to normal operation (23-24). However, for new vehicles low mass and number emissions have been shown (20,25). Controversy over emissions remains because new SI vehicles are not necessarily representative of those operating on-road and because laboratory tests may or may not be representative of real-world operating and environmental conditions.

Diesel Engine Emissions

Michigan Technological University (MTU) evaluated the impact of low-emission engine technology on diesel particulate matter (DPM) emissions (13,26) in the laboratory. The engine had a high pressure, mechanically controlled, fuel-injection system, and other design features now commonly used in heavy-duty, high-speed, on-highway diesel engines. MTU showed that this technology significantly reduced mass emissions, but caused a prominent shift in the size distribution of DPM towards smaller nuclei-mode particles when compared to emissions from an older engine.

Under steady-state conditions, the modern engine produced up to 40 % of the particle volume in the nuclei mode range. Previous studies (23, 27-29) reported 1-20 % of the mass in

this range. The major difference between the modern and older engines evaluated at MTU was the fuel injection system. The modern engine incorporated a high-pressure fuel-injection system that injected fuel at 1,520 bar compared to 1,240 bar for the older engine. [A bar is a unit of pressure and is equal to 0.987 atmosphere.] MTU postulated that the higher injection pressure created more solid, nuclei mode particles, which were not removed by an oxidation catalytic converter. MTU and the Health Effects Institute (HEI) consider the particle size distribution findings preliminary in nature, and HEI recommended the findings be verified with representative engines from different manufacturers.

Work in our laboratory (30) suggests a different interpretation. High nanoparticle emissions are not necessarily the result of high injection pressure. We believe that higher nanoparticle emissions are a consequence of reducing the mass of particles in the accumulation mode compared to the mass of semi-volatile material likely to become solid or liquid by homogeneous nucleation or condensation/adsorption as the products of combustion expand and cool and then dilute and cool. The driving force for gas-to-particle conversion processes is the saturation ratio, S, the ratio of the partial pressure of a nucleating species to its vapor pressure. For materials like the constituents of the soluble organic fraction (SOF) or sulfuric acid, the maximum saturation ratio is achieved during dilution and cooling of the exhaust (31), and typically occurs at dilution ratios between about 5 and 30. The relative rates of nucleation and condensation/adsorption are an extremely nonlinear function of S. Low values of S favor adsorption/condensation, high values nucleation. The rate of adsorption/condensation is proportional to the surface area of particulate matter already present (32-33). Thus, the large mass, and consequently surface area, of soot agglomerates present in the exhaust of old technology engines will take up supersaturated vapors quickly and prevent S from rising high

enough to produce nucleation. On the other hand, in a modern low emission engine there is little soot surface area available to adsorb or condense supersaturated vapors making nucleation more likely. This will be especially true if the solid carbon emissions have been reduced relatively more than sulfuric acid and material that makes up the SOF. Our view is supported by a study of the influence of injection pressure on particle mass and number emissions in the 400 to 1000 bar range that showed a continuous decrease in both mass and number emissions with increasing pressure (34).

The engine used at MTU emitted low concentrations of particles in the accumulation mode diameter range, where soot agglomerates reside, and had a very high percentage of soluble SOF ranging from 60 to 75 %. These factors would favor nucleation of the SOF as nanoparticles. The high fuel injection pressure and the fuel-air mixing strategy used in their engine probably led to more effective reduction of soot than SOF. Thus, the high injection pressure indirectly led to an increase in number emissions. However, other engine modifications or aftertreatment devices that reduce soot emissions more effectively than SOF or sulfuric acid are also likely to increase particle number emissions. In fact, this was exactly what has been observed downstream of some trap oxidizer systems (35-36).

The same arguments just made about the role of soot agglomerates in suppressing nucleation during dilution and cooling of the exhaust also apply to nucleation of ash constituents that are volatilized at combustion temperatures, except that in the case of ash constituents the nucleation takes place inside the engine during the expansion stroke immediately after combustion. We use the term ash to describe inorganic solid materials present in exhaust particulate matter (including for example metal sulfates and oxides). Prior to our recent work and similar work in Switzerland (37), we had not seen evidence of significant solid ash particle

nucleation except when high concentrations of metals were added with fuel additives. Our tests using a Perkins diesel engine suggest that soot emissions may have been reduced to such a low level that the agglomerates no longer provide enough surface area to relieve ash supersaturation and prevent nucleation of ash derived from lube oil. Once ash nuclei are formed they may serve as heterogeneous nucleation sites for SOF and other species during dilution and cooling of the exhaust. In some cases the particles in the high SOF nuclei mode observed in the past may have had ash cores.

Thus, the nanoparticles observed in the diluted exhaust of low emission diesel engines may consist of solid carbon or ash particles, semi-volatile nuclei formed by homogeneous nucleation or semi-volatile nuclei with a solid core formed by heterogeneous nucleation on existing particles. It is clear that a number of factors affect the fine particle aerosol size distributions, and if not properly understood and accounted for in the laboratory, can create a laboratory aerosol artifact that is not representative of concentrations in the ambient environment. Representative measurements of such particles can be made only if the sampling and dilution system simulates atmospheric dilution to the extent necessary to reproduce size distributions observed under atmospheric dilution conditions. Regardless of how particles are formed, the relationships between lab and atmospheric dilution ratio, dilution rate, saturation ratio and the other processes affecting particle formation must be understood. In another study (38) that used the same type of engine used in our lab (31), it was reported that the particle size distributions and number concentrations were significantly affected by dilution conditions. We have also observed that dilution conditions significantly affect particle formation.

The residence time of particles in the atmosphere is particularly important because it impacts what particles are available for inhalation and deposition. The typical residence time for

10 nm particles is quite short, on the order of minutes (39), because these particles diffuse to and coagulate with larger accumulation mode particles. Although their individual particle identity is lost, these particles remain in the atmosphere as part of larger particles, which coincidentally have lower alveolar deposition rates. Particles in the 0.1 – 10 μm diameter range have a much longer residence time, on the order of days, while larger particles are removed from the atmosphere quite quickly by gravitational settling and impaction on surfaces.

Uncertainty exists regarding the relative contribution of atmospheric aerosol from SI and diesel exhaust in real-world conditions. Diesels emit more particulate matter on a fleet average, gram-per-vehicle mile mass basis, but because SI vehicles, at least in the U.S., account for most of the vehicles operating on-road, the direct PM emissions from SI engines may be more important. The Northern Front Range Air Quality Study (40-41) found that vehicle exhaust was the largest PM2.5 total carbon (TC) contributor, constituting about 85 % of PM2.5 carbon at sites in the Denver metropolitan area. Sources with emissions similar to light duty gasoline vehicles contributed about 60 % of PM2.5 TC at urban Denver sites, and these contributions were 2.5 -3 times the diesel exhaust contributions. Emissions were particularly high during cold, cold starts and from vehicles identified as "smokers". A cold, cold start occurs when the engine temperature is $< 0^{o}$ C (32^{o} F). However, diesels contributed the largest share of the "elemental" carbon (EC) at these locations.

CHAPTER 2
MEL AND INSTRUMENTATION

The UMN MEL was used to collect gaseous and particulate matter data while it was operated on Minnesota roadways. Figure 3 is a schematic diagram showing the sample flow and instruments in the MEL. Sampled aerosol was transferred to the UMN Mobile Emissions Laboratory (MEL) through an 8.9-cm (3.5 in) diameter metal pipe that protruded 43-cm (17 in) in front of the MEL and 61-cm (2 ft) above the ground. The metal pipe was connected to about 9-m (29.5 ft) of flexible tubing that carried the aerosol from the point the sample was collected in front of the Volvo tractor to the point where it entered the MEL. Total sample line length was less than 11-m (36 ft) with a flow rate of 350 lpm (12.4 cfm).

The MEL manifold shown in figure 3 distributes sample to the instruments. The MEL also contains a bag sampler that is shown schematically in figure 4. The bag sampler was housed in a 208 L (55 gal) drum. The drum held an electrically conductive bag (Associated Bag Co, Milwaukee, WI) that was filled either from sample air or with air filtered through an absolute filter (Donaldson, Co., Minneapolis, MN). To obtain a bag sample the bag was purged, filled with clean air, purged and filled with sample air. A bag sample permits a size distribution to be obtained from a grab sample of air collected in the bag as opposed to a continuous stream of air flowing though the sampling manifold. A bag sample represents a discrete sample collected over a 5.5 s window of time (time required to fill the bag) that changes slowly over time. Aerosol decay in the bag sample is a primarily a function of particle losses within the bag. Particle losses in the bag during a normal sampling cycle are about 10 %.

The MEL has a suite of aerosol instrumentation capable of sizing diesel aerosol from <

10 nm - 10 μm in near real-time. The particle size instruments include an electrical low-pressure impactor (ELPI), a scanning mobility particle sizer (SMPS). In addition to these instruments, other real-time instruments are available to measure other aerosol characteristics. A photoelectric aerosol sensor (PAS) measures surface-bound polycyclic aromatic hydrocarbons and a diffusion charger (DC) provides an estimate of surface area. The DC is particularly useful because of its fast response. The primary aerosol instruments used to determine the size distribution in near real-time are the ELPI and SMPS. An Ultrafine Condensation Particle Counter (CPC) combined with a leaky-filter dilutor was used to determine total particle counts. The CPC has a maximum concentration of 100,000 particles/cm^3 and a dilutor was necessary to reduce the aerosol concentration to within operating limits of the CPC. The leaky-filter dilutor design was chosen because of its repeatable dilution and simple design.

The leaky filter dilutor works passively and is therefore dependent upon the flow rate generated by the measurement instrument. A glass capillary tube was placed inside each of two capsule filters (No. 12144, Pall-Gelman Laboratory) to create a leak through the filter. The diameter of the capillary tube determines the dilution ratio. Figure 5 is a schematic diagram of one leaky filter dilutor. In our application two leaky filters connected by a Tygon tube were used in series to obtain a high enough dilution ratio for the Ultrafine Condensation Particle Counter.

The dilution ratio, D_r, is defined as

$$D_r = \frac{C_0}{C_{dil}}, \tag{0.1}$$

where C_0 and C_{dil} are the initial and diluted concentrations, respectively. The diluted concentration is defined as

$$C_{Dil} = \frac{C_0 Q_{cap} + C_{fil} Q_{fil}}{Q_{inst}}, \tag{0.2}$$

where C_{fil} is the filtered concentration, Q_{cap} is the capillary aerosol flow rate, Q_{fil} is the filtered aerosol flow rate, and Q_{inst} is the measurement instrument flow rate. Since the filtered aerosol concentration is essentially zero, $C_{fil} = 0$, we have

$$C_{Dil} = C_0 \frac{Q_{cap}}{Q_{inst}}. \tag{0.3}$$

Substituting C_{dil} into (0.1), the final dilution ratio is

$$D_r = \frac{Q_{inst}}{Q_{cap}}. \tag{0.4}$$

The pressure vs. flow relationship of the capsule filter was measured. The results were approximated by a linear regression to obtain an empirical relation for the filter pressure vs. flow such that

$$\Delta p_{fil} = m Q_{inst} \tag{0.5}$$

where ΔP_{fil} is the pressure drop across the filter and m is the measured slope. The pressure drop across the capillary is related to the flow rate by

$$\Delta p_{cap} = \frac{128 Q_{cap} \mu L}{\pi d^4}. \tag{0.6}$$

where

Δp_{fil} = pressure drop

μ = gas viscosity = 1.83×10^{-4} g/cm-s

L = capillary length [cm] and

d = capillary diameter [cm].

Equation (0.6) is the Hagen-Poiselle equation of laminar flow through a pipe (42). The pressure drop across the capillary and the filter are nearly equal; thus setting equations (0.5) and (0.6) equal and substituting equation (0.4) gives

$$d = \left(\frac{128 Q_{cap} \mu L}{\pi m Q_{inst}} \right)^{1/4} = \left(\frac{128 \mu L}{\pi m D_r} \right)^{1/4} \qquad (0.7)$$

The capillaries were made at the UMN glass blowing shop. The most suitable diameter available was 0.2 cm to attain a dilution ratio, D_r, between 14 and 16:1. Total dilution was measured experimentally and estimated to be 220:1. However, the dilution ratio is affected by particle size and a full characterization of the two leaky filters has not been completed at this time. However, based upon our field experiments we believe that the 220:1 dilution ratio used herein is a reasonable estimate. Further characterization of the leaky filters is ongoing.

The SMPS was operated using sample either from the bag or sample brought through the sampling system on a continuous basis. When the SMPS obtains a sample on a continuous basis, the aerosol sample changes constantly over time but covers a wide window in time. The magnitude of change during a continuous SMPS scan is a function of the sample source. On the other hand, when the sample was obtained from the bag, the sample source remains constant during analysis but covers a narrow 5.5 s window of time, the time required to fill the sampling bag. Most of the size distributions shown later were determined by averaging distributions from

the SMPS while it was obtaining a continuous sample.

The MEL is also equipped with three-gas analyzers: a non-dispersive infrared (NDIR) CO_2 analyzer, a NDIR CO analyzer and a chemiluminescence NOx analyzer. Each of the instruments has several concentration ranges. For this study, the range of the CO_2 analyzer was 0 - 2500 parts per million (ppm). The CO analyzer was 0 –1100 ppm, and the range for the NOx analyzer was 0 - 10 ppm. These instruments have a response time of about 1 s and are used to determine the dilution ratio of the aerosol plume and fuel specific emissions.

Two laptop computers logged data from the instruments using a National Instruments Labview based data acquisition system. Power was supplied to the laboratory by two Onan diesel generators. Weather data were obtained using a Kestrel 3000 pocket weather meter (Nielsen-Kellerman, Chester, PA) and the local radio. Computer clocks were synchronized using a Synctime clock (Acron Time Technology, Oak Brook, IL). A video camera located in the cab of the Volvo was used to record traffic activity in front of the MEL. The video camera was connected to a TV in the MEL to provide the operator of the MEL instruments a forward view of the road ahead. Personal hand held radios provided communication between the Volvo cab and the MEL operator.

CHAPTER 3
METHOD AND APPROACH

Each instrument in the MEL has a check sheet that is used daily to assist the operator maintain quality assurance (QA). These sheets were developed prior to the start of this project as part of the CRC E-43 project QA program. They insure that important instrument parameters are recorded prior to the beginning of each sampling day and that problems are recorded.

Each day the gas and particle instruments were warmed up for about 1-hr and calibrated. Gas instruments were zeroed and spanned using NIST traceable calibration gases and pure nitrogen as the zero gas. Figure 6 is a strip chart showing the gas instrument calibration done on the morning of November 10, 2000.

An absolute filter was used to zero the aerosol instruments and ammonium sulfate aerosol was nebulized to check the day-to-day particle size consistency for the SMPS and ELPI. We also compared the CPC, SMPS, ELPI and DC response to see that they were in the normal range of operation. Figures 7 and 8 show the average ammonium sulfate and absolute filter zero calibrations. All flows were checked using a bubble meter (Gillian Gilibrator, Sensidyne, Clearwater, FL). Figure 7 shows that although the ammonium sulfate aerosol concentration varies day-to-day, the mode lies between 30 to 35 nm and is quite consistent. Day-to-day variation in ammonium sulfate concentration is expected and is not part of the consistency check. Figure 9 shows a comparison between the SMPS and ELPI. The size distributions are quite different because the principle of operation and size ranges of the two instruments are different. The SMPS covers the range from about 8 nm to 300 nm while the ELPI covers the range from 30 nm to 10 μm.

In addition to the instrument check sheets, the MEL operator and the project leader riding in the cab of the Volvo maintained SMPS and event logs. The MEL operator recorded SMPS and continuous instrument information such as date, scan time, scan filename, scan quality, continuous data file name and file start and stop times. The project leader also recorded this information as well as information on the Volvo's speed, location, traffic conditions, weather, the presence of diesel traffic and other pertinent information. This information was electronically transcribed and coded and associated with the raw data obtained by the instruments. Date and time stamps in the electronically recorded instrument data were used to associate these data with information transcribed in the logs and later coded into the electronic records.

Coding data requires judgment, because the Volvo's speed, traffic conditions, and the presence of diesel vehicles were not continuously recorded electronically. In particular, since the SMPS was operated primarily in the continuous scan mode while on the highway, the presence of a diesel vehicle(s) in front of the MEL was coded over a window of time, because the SMPS records data over a 90-s period. For instance, if a diesel truck passed the MEL at 13:00:00, and an SMPS scan began at 12:59:15, the diesel was assumed to have passed while the SMPS was scanning because the scan would have begun at 12:59:15 and ended at 13:00:45. The diesel plume may have impacted the size distribution. Therefore, even though the diesel truck may have passed the MEL at a specific time, the impact of that plume on the SMPS size distribution may occur anytime during that SMPS scan. The impact is limited to the SMPS channels being scanned when the diesel truck passes. Similarly, the Volvo speed was recorded periodically. It was assumed that the same speed was maintained from one log entry to the next. Coding is more precise for the continuously recording instruments that record a data point about every second.

More information can be obtained from the videotapes; however, it was not possible to continuously time stamp the videotape. Periodically a clock was held in front of the video camera, and further synchronization is obtained by comparing the hand written logs to specific events on the tape such as the passage of a smoking bus at a specific location and time. Interesting or difficult to interpret events can be viewed on the tapes, but viewing the videotapes to enhance the hand written logs is very time consuming.

Table 1 shows a small portion of coded data from an SMPS data file. The SMPS scan type refers to either a continuous scan (C) or a scan taken after a bag fill (B). In this case all the scans were continuous except for when the Volvo passed through the Lowry Tunnel and the bag was filled. The approximate location, Volvo speed and the presence of diesel traffic are recorded with more exact information recorded in the hand written log. The SMPS scan time refers to the time when the SMPS began a size distribution scan. This portion of the log shows that a bag sample was collected in the Lowry Hill Tunnel.

Figure 10 is a map that shows the route taken by the MEL while sampling on-road. These routes were selected because they represented a mixture of county and interstate highways that had high volumes of traffic during the day. The route marked in red was traveled on November 2, 3 and 9, 2000 and the green route was traveled on November 10 and 15, 2000. Stationary sampling points were selected north and south of Highway 62 (also known as Crosstown Highway) just west of the Portland Ave exit about 10 m from the highway and residential homes and east and west of 494 and County Road 9 (Rockford Rd) about 500-700 m from the I-494 in residential areas. Stationary samples were also collected at a Holiday gas station located in the northwest corner of the I-694 and County Road 47 exit. Sampling was also conducted as the MEL passed through the Lowry Hill Tunnel in downtown Minneapolis.

Date	SMPS scan type	Volvo location	Diesel traffic	Volvo speed, mph	SMPS scan time
11/15/2000	C	Cedar Bridge N	N	60	13:18:10
11/15/2000	C	Cedar N	Y	60	13:19:39
11/15/2000	C	Cedar N	Y	30	13:21:09
11/15/2000	C	Cedar N	N	3	13:22:39
11/15/2000	C	Cedar N	N	30	13:24:09
11/15/2000	C	Cedar N	N	35	13:25:39
11/15/2000	C	62 W	N	50	13:27:09
11/15/2000	C	35 N	Y	55	13:28:39
11/15/2000	C	35 N	Y	55	13:30:09
11/15/2000	C	35 N	Y	55	13:31:39
11/15/2000	C	35 N	Y	55	13:33:09
11/15/2000	B	Lowry tunnel N	N	50	13:35:58
11/15/2000	C	94 W	Y	55	13:38:04
11/15/2000	C	94 W	N	55	13:39:33
11/15/2000	C	94 W	Y	55	13:41:03
11/15/2000	C	94 W	N	55	13:42:33
11/15/2000	C	694 E and University	N	20	13:44:03
11/15/2000	C	47 N	N	20	13:45:33
11/15/2000	C	Holiday station	N	0	13:47:03
11/15/2000	C	Holiday station	N	0	13:48:33
11/15/2000	C	Holiday station	N	0	13:50:03
11/15/2000	C	Holiday station	N	0	13:51:33
11/15/2000	C	Holiday station	N	0	13:53:03
11/15/2000	C	Holiday station	N	0	13:54:33
11/15/2000	C	Holiday station	N	0	13:56:03
11/15/2000	C	Holiday station	N	0	13:57:33
11/15/2000	C	Holiday station	N	0	13:59:03
11/15/2000	C	Holiday station	N	0	14:00:43
11/15/2000	C	Holiday station	N	0	14:02:12
11/15/2000	C	Holiday station	N	0	14:03:42
11/15/2000	C	Holiday station	N	0	14:05:12
11/15/2000	C	47 S	N	20	14:06:42
11/15/2000	C	694 W	N	60	14:08:11

Table 1. Sample SMPS electronic file

The MEL covered about 500 miles over the five days of sampling and encountered a variety of traffic conditions from bumper to bumper traffic jams to high speed, free flowing traffic. An effort was made by the MEL driver to maintain at least 10-m between the MEL and the vehicle in front, and no attempts were made to capture a vehicle plume. Since the sampling probe was close to the highway it is assumed that exhaust from trucks with high exhaust stacks would only be sampled after thorough mixing. Stratification of the aerosol on the highway would have favored sampling emissions from low exhaust mounted vehicles that are predominately gasoline fueled.

Samples were also collected at a metered ramp on July 6, 2000. The ramp was located in the NE corner of the I-494 and County Road 169 intersection. Ramp sampling required prior approval by the Minnesota Department of Transportation, 24 hr prior notification, and once the MEL was in place it could not be moved until the end of the rush hour. Ramp sampling was attempted on other occasions but either the wind or traffic were going in the wrong direction and the impact of emissions on air quality was not determined.

CHAPTER 4
RESULTS AND DISCUSSION

The objective of this project was to obtain size distribution and number concentration data to characterize Minnesota roadway aerosol with an emphasis on nanoparticles. Nanoparticles are less than 50 nm in size and the two instruments best able to measure these particles are the SMPS and the CPC. The SMPS, as configured in this study, sizes particles in the 8 to 300 nm range and can be used either in the continuous scanning mode, where sample is continuously obtained from the sample stream, or to obtain a sample directly from a bag. Number, volume and surface area distributions can be obtained from the SMPS. The CPC counts all particles greater than about 3 nm. The integrated SMPS number count can be compared to the total CPC particle count, but these counts may differ depending upon the number of particles that fall outside the range of the SMPS instrument, particle losses within the instruments and the losses that occur within the CPC dilutor. The ELPI also can be used to obtain size distribution and number data. However, the ELPI has a lower limit of 30 nm. The total number concentration of particle (particles/cm^3) obtained from these instruments should track each other over time. This is the case as seen in the strip chart data discussed below.

Particle Number Concentration Strip Charts

Results from the continuously recording instruments (CPC, ELPI, NOx, CO and CO_2) are best viewed as strip charts that cover the entire daily sampling period. The integrated number concentration obtained from each SMPS scan can also be plotted on these charts. Each SMPS point represents a 90 s window in which the SMPS was scanning on a continuous basis to complete a size distribution. By narrowing the time window of the chart by reducing the time

period covered on the x-axis, and by adjusting the scale on the y-axes specific events recorded in the log can be examined more closely. The strip charts are most easily viewed when separated into gas and particle charts by day.

Figures 11 through 24 are strip charts showing the CPC, ELPI and SMPS particle number concentration (particles/cm^3) and Volvo speed as a function of time. It would be expected that the CPC would have the highest concentration of particles, and the ELPI the lowest, because of the dynamic ranges of each instrument. This was found to be the case. Speed is shown on the graphs as an indicator of traffic volume; the slower the speed the more congested the area, or the slower the speed limit if the Volvo was in a residential area. Speed is also an indicator of the load being placed on the engine. The higher the speed the greater the particulate emissions as discussed earlier. Further, colder ambient temperatures lead to more nanoparticle formation and data shown in the charts were collected in November 2000 at temperatures between 1-13^o C and relative humidity between 40 and 60 %.

Figures 11 to 13 show data collected on November 2, 2000. The red route shown on figure 10 was followed. On figure 11 CPC particle concentrations range from 10^4 to over 10^6 particles/cm^3 for the entire sampling period. During the period from 13:40 to 14:40, no CPC data were collected due to a computer crash in the MEL. Periods of computer outage or other instrument problems are indicated by straight lines and in most cases are denoted on the graphs with a note and arrow. In general, higher speeds are associated with higher particle counts, and this is evident throughout the charts.

One of the goals of the study was to examine the impact of highway traffic on residential areas. Four locations were selected for this portion of the study. Two locations were located north and south of Highway 62 just west of Portland Avenue at 62nd street north or south and 4th

avenue. The nearest homes in these areas are about 20 m from the highway. Figure 12 is the first of four figures 15, 16 and 19 are the others that show data collected at 62nd street north and south and 4th avenue. The MEL was parked in the same locations each day about equidistant from the highway and the homes. On November 2 the MEL was also parked at 2nd avenue and 60th just below I-35 W and this is shown on figure 12. Traffic on I-35 W impacts air quality in this residential area when the wind is from the NW, W or SW because of its proximity to the Highway 62 and the I-35 W split. From figures 12, 15, 16 and 19 it can be seen that particle number concentrations are generally between 10^4 and 10^5 particles/cm^3, with higher concentrations tending to be later in the day beginning around 15:00 when rush hour traffic begins to pick up. There was no clear cut upwind and downwind at these locations because the wind varied from the W, NW, but in general, homes on the north side of Highway 62 had lower particle number concentrations. This is affirmed by the gaseous strip chart data shown later.

Traffic on Highway 62 was moderate to heavy during the times we were sampling. During the sampling periods, one-minute car and truck counts were taken on numerous occasions. On average 56 cars and 3 trucks passed our location in one minute. This car count is for one direction only; therefore, assuming no difference in the traffic volume in the other direction, the total count would be 112 and 6 over a one-minute period.

Figure 13 shows a period of time when the Volvo was in a traffic jam heading east on Highway 62. Particle number concentrations are lower ranging from 10^3 to 10^5. This agrees with what is known about particle emissions, lower engine load and speed produce lower particle emissions. Note the agreement between the ELPI, CPC and SMPS is quite good suggesting that the particles are generally larger within the dynamic range of both instruments. This is affirmed by the size distributions shown later.

Figures 14 through 16 show particle number concentration data for November 3, 2000 when the red route shown in figure 10 was again followed. Figure 14 is the chart for the entire sampling day and figures 15 and 16 are for periods when the Volvo was parked north and south of Highway 62 in the residential areas. Note that the orientation of the MEL was different for figures 15 and 16. On figure 15 the MEL first parked north of Highway 62 and then moved to the southern position. On figure 16 the parked position and times are reversed. On figure 15 and 16 there are periods of time when the SMPS integrated particle number concentration is lower than the CPC concentration. We believe this discrepancy is related to the fact that the CPC counts particles below the range of the SMPS. This discrepancy is also observed when the Volvo is traveling at higher speeds when more particles are produced. Correcting for these differences would increase the particle count that is the SMPS is under estimating the true particle count.

Figures 17 through 19 show data collected on November 9, 2000 while the Volvo was on the red route. Figure 17 is the plot for the entire sampling day. Figure 18 shows number concentrations when the Volvo was running a various speeds. During periods when the traffic was slowed due to traffic congestion, the total number counts were lower and there was better agreement between the SMPS and CPC. Higher speeds resulted in higher particle number concentrations and less agreement between the two instruments, which is expected.

On November 10 and 15, 2000 the Volvo traveled the green route shown in figure 10. This route differed from the red route in that it was observed to have a higher volume of diesel vehicles and because it was nearly entirely interstate highway. Stationary samples were collected east and west of I-494 at Rockford road. The arrow in figure 10 labeled 23 in Plymouth, MN indicates the general location. These samples were between 500 and 700 m (0.3

to 0.4 mi) from the highway at Fernbrooke and 42nd west of I-494 and 42nd and NW Blvd east of I-494. Both sampling sites were located on streets in upscale neighborhoods.

Figures 20 and 21 show data from the CPC, ELPI and SMPS collected on November 10, 2000. Concentrations on the highway range between 10^4 and 10^6 particles/cm^3, and are similar to the concentrations found on the red route. Particle number concentrations found in the two residential areas are much lower than those measured at the Highway 62 locations. The wind direction was from the west, and figure 21 illustrates that concentrations downwind or east of I-494 were slightly higher than the upwind concentrations. Nanoparticles have a relatively short life in the atmosphere on the order of a few minutes as they merge to form larger particles through a number of processes, but the major effect here is probably dilution of the concentration. It is interesting to note how quickly these concentrations rise as the Volvo approaches and crosses I-494 at Rockford Road (County Road 9). This increase is in part due to traffic on County Road 9 and in part due to exhaust emissions from I-494.

Figures 22 through 24 show data from November 15, 2000. Concentrations are similar to November 10. Figure 23 shows that concentrations downwind or east of I-494 are somewhat higher than the upwind concentrations and that these concentrations increase dramatically as the Volvo approaches and crosses I-494 at Rockford Rd. Figure 24 shows concentrations at different speeds and again higher concentrations are associated with higher speeds and better agreement between the SMPS and CPC are observed at lower speeds.

Gas Concentration Strip Charts

Figures 25 through 36 show the gas data for the five sampling days described previously. Several points of clarification will assist the reader. The carbon monoxide (CO) and carbon

dioxide (CO_2) instruments record on the parts per million (ppm) scale while the oxides of nitrogen (NOx) analyzer records on the parts per billion (ppb) scale. The CO analyzer has a high and low range and on November 2 it can be seen that the maximum reading was 100 ppm indicating that it was on the low range and the maximum concentration was recorded. On subsequent days the range was adjusted to the high range 0 to 1100 ppm to avoid this problem. The normal background concentration of CO_2 is 350 ppm (43). Minimal background concentrations of CO and NOx are expected. The gas data are useful in estimating fuel specific emissions. Fuel specific emissions estimate the amount of particulate pollution attributable to highway traffic.

SMPS Size Distributions

The SMPS data are shown as average size distributions grouped by condition such as vehicle speed, location and the presence of diesel vehicles during the scan. The unit of the y-axis is the differential number (or volume) of particles per differential log diameter within an interval of the size distribution (dN/dlogDp or dV/dlogDp) where N is particle number (or V is volume) and Dp is the particle diameter. When data are plotted in this way, the area under the curve gives the number (or volume) of particles in that size range when the y-axis is on a linear scale. The distributions are shown (figures 37-50) without error bars because of the difficulty of reading the charts when the bars are present. The sample standard deviations, which estimate the population standard deviation, are large and tend to overlap from one distribution to the next. Figure 7 shows the error bars for calibration aerosol. Further the sample standard deviation measures the variability in concentration within a size range in the SMPS. The concentration of a given particle size tends to fluctuate widely due to different dilution conditions, background levels and

other causes. A better estimate for our purposes is the standard deviation of the mean derived by dividing the sample standard deviation by the square root of the number of samples. This gives a measure of the standard deviation of the mean for a size distribution. These values can be calculated from the data.

Figures 37, 39, 41 show number size distributions averaged by conditions of speed, interstate and County Road and the presence or absence of diesel vehicles. Figures 38, 40 and 42 show the corresponding volume distributions. Speed appears to have a dramatic effect on the nuclei mode and nanoparticle formation. Note the large peaks in figure 37 compared to figure 39. In figure 37 the peaks are between 10 – 12 nm and the minimum peak concentration is 200,000 particles/cm^3. Note that three of the distributions suggest that a second mode might be forming to the left below the range of the SMPS. This is consistent with the findings of the CPC recording higher concentrations than the SMPS at higher speeds. Contrast this to figure 39 where only one peak is distinctly present for the case when diesel trucks were in the vicinity of the MEL and this peak is between 28-30 nm. Under low engine speed and load less particulate material is present in the exhaust. On the other hand the shape of the volume distributions is similar regardless of speed. Most aerosol mass or volume consists of large particles found in the accumulation mode (see figure 3). As the particles in the nuclei mode age they increase in particle size through coagulation, agglomeration, adsorption and other processes to become accumulation mode particles. Notice that the volume concentration is higher under the low speed and load condition. This is consistent with the idea that the aerosol is aging in stagnant traffic conditions and becoming larger in size. Additional data need to be collected to confirm these findings.

Figures 41 and 42 are summary graphs for number and volume by speed regardless of

road type or the presence of diesel vehicles. The number and volume of particles vary inversely when speed is the grouping variable. As speed increases, the number of nanoparticles increases but the volume of particles decreases.

Figures 43 and 44 show the number and volume distributions for SMPS data collected while the Volvo was moving on local roads prior to stopping in the residential areas. In each graph, two size distributions are shown, one includes all data and the other excludes data with unusually high number concentrations. The number distributions are bimodal with peaks around 20 and 60 nm, indicating the presence of fresh and aged aerosol from different sources. The volume distributions are similar to the on-road measurements previously mentioned. The volume distributions suggest we are only measuring part of the accumulation mode as defined in figure 2. The upper end of this mode could have been measured if the SMPS had been set to 100 pct of full scale with an upper limit of 700 nm but in that case information would have been lost on the lower end where most of the nanoparticles are found.

Figures 45 through 47 show the number and volume distributions for the SMPS scans taken while the Volvo was parked either in a residential area or at the Holiday gas station. Note that the number distributions are quite different for the Highway 62 and County Road 9 positions. The closer a home is to a main road the higher the nanoparticle concentration and the smaller the particles. The shapes of the volume distributions; however, are essentially identical. The Holiday gas station concentrations are higher reflecting the close proximity of the MEL to automobiles entering and leaving the gas station. However, none of these vehicles were parked in front of the MEL.

Figure 48 shows the average results of four SMPS scans completed on bag samples collected in the Lowry Tunnel. These data were taken from bag samples collected in the middle

of the Lowry Tunnel. Three samples were collected while traveling northbound and one while traveling southbound. Nanoparticle concentration ranged from 150,000 to more than 600,000 particles/cm^3 and this is reflected in the height of the error bars.

Metered Ramp Sampling

Prior to the on-road sampling an effort was made to sample at metered and non-metered ramps. For this portion of the study, a portable sampling tube was constructed of flexible exhaust tubing that extended to the meter. Locations were pre-selected with the assistance of MnDOT and arrangements were made 24 hr in advance of the sampling. The MEL would move into a location and not move again until the rush hour subsided. If the wind direction or traffic was not in the right direction, sampling was not successful.

Data were collected on July 6, 2000 and the results are shown in figures 49-52. Figure 49 shows the average SMPS number and volume size distributions for about 150 min of sampling from just before 16:00 to just after 18:15. Note the height of the error bars that show a great fluctuation in the aerosol concentration. The number mode is around 50 nm and the aerosol is much larger in size than what was observed on-road. The size distribution is unusual in that the aerosol is large in size. It is possible that the orientation of the MEL in relationship to the wind direction allowed exhaust from the two diesel generators used to power the lab to enter the sample stream. However, project staff did not note this condition in the log.

Figures 50 through 52 display the time series size distributions. Figure 50 shows each number distribution individually and figures 51 show number and volume distributions grouped into approximately 15-minute periods. The size distribution does shift over time and a nuclei mode is apparent around 17:00 in figure 50. In general, as the rush hour progresses both the

number and volume distributions have modes with smaller particle size.

Fuel Specific Particulate Matter Emissions

Emission factor estimates can be derived from our data. For these calculations, background and on-road levels of CO, CO_2 and particles must be determined. We present estimates for the 10th and 15th of November when the Volvo traveled the green route. Our estimates are for a gasoline vehicle dominated scenario. Background levels were determined by averaging the concentrations obtained when the Volvo was parked either at Fernbrooke and 42nd W of I-494 at Rockford Rd or at 42nd Place and Northwest Blvd. E of I-494. The highway concentrations were obtained from data collected on I-494 N and S of Rockford Road. The highway estimates are broken into groups based upon the location of the Volvo either N or S of Rockford Rd. and the speed of the MEL. A mass balance equation is used to derive the estimates. The first step is to determine the ratio of particles to carbon added by the highway traffic.

1. Particles/ Mass of Carbon = $$\frac{(\text{particles/cm}^3)(10^6\ \text{cm}^3/\text{m}^3))}{((CO_{avg} + CO_{2\ avg})(M_C / M_{air})(\text{Density air}))}$$

Where M_c and M_{air} are the molecular masses of carbon and air, 12.01 and 29.97, respectively, CO and CO_2 are expressed as mole fractions, density air = 1.18 kg/m^3. All concentrations are those added by vehicles, i.e. roadway – background. It is assumed that all of the carbon added by the highway is in the form of CO_2 and CO. This is a reasonable assumption since gasoline engine combustion efficiencies are better than 90 % (44), thus more than 90 % of the carbon in the fuel is converted to CO_2 and most of the incompletely burned carbon leaves as CO. This is illustrated by the Federal tailpipe new vehicle emission standards that all nearly ten 10 times the amount of CO compared HC, 3.4 g/mi versus 0.41 g/mi. The particles/mass of carbon may be

converted to particles / mass of fuel if the carbon content of the fuel is known.

2. Particles/Mass of Fuel = (Particles/Mass of Carbon)(Mass Fraction Carbon in the Fuel)

The carbon content of gasoline ranges from 0.83 to 0.86 as a mass fraction (45). For the previous calculations, 0.85 was used. Equations 1 and 2 yield the fuel specific emissions in particles/kg of fuel. Emissions expressed in this form are especially useful if total fuel consumption by a vehicle fleet is known. These results may also be used to estimate particle emissions in particles/mile assuming vehicle fleet average fuel consumption. For our calculations, we assumed average fuel consumption to be 20 MPG and average fuel density to be 2.8 kg/gal for gasoline (46). This yields 7.1 miles/kg. Dividing particles/kg by miles/kg yields particles per mile.

Table 2 shows the on-road data used to obtain the estimates of fuel specific particle emissions and tables 3 and 4 show the fuel specific emission estimates derived from the CPC and SMPS average number concentrations. No particle/mi estimate is shown for the traffic jam because of the very slow highway traffic speed. The background values for gases and particulate matter used to derive the fuel specific particle emissions are derived from data in table 2. They are the averages of the values obtained at Fernbrooke and 42nd west of I-494 and 42nd Place east of I-494. Although the upwind values obtained west of I-494 were somewhat lower it was decided to average the values together to obtain the overall average background. Average background values were obtained for both the 10th and 15th of November.

Table 2. On-road data used for fuel specific and particle/mi number emissions

Date	Time		Location	Speed mph	$CO + CO_2$ ppm		CPC * 220 part/cm^3		SMPS Cont part/cm^3		SMPS Bag part/cm^3	
	From	To		Mean	Mean	SD	Mean	SD	Mean	SD	Mean	SD
11/10/00	14:46	15:00	Fernbrooke and 42nd	0	368	5	1100	440	1900	300	1500	300
11/10/00	15:14	15:32	42nd Place	0	368	6	9500	2900	7400	3600	4600	1100
11/10/00	15:38	15:51	I-494 going S	46	421	47	72000	73000	35200	19000		
11/10/00	15:51	16:39	I-494 going S Traffic Jam	9	420	44	90600	417000	93000	82000		
11/10/00	16:39	16:48	I-494 going E	40	488	41	238000	149000	220000	82000		
11/15/00	14:17	14:20	I-494 going S	59	412	75	274000	252000	82000	106000		
11/15/00	14:24	14:39	Fernbrooke and 42nd	0	362	7	9700	11000	14200	12000	11600	2700
11/15/00	14:51	15:08	42nd Place	0	363	12	16300	7700	10800	3200	12500	300
11/15/00	15:09	15:29	I-494 going S	44	415	55	350000	345000	89000	69700		

Table 3. On-road fuel specific and particle/mi estimates derived from the CPC and SMPS

Date	Time		Location	CPC	SMPS	CPC	SMPS
	From	To		Part/mile	Part/mile	Part/kg fuel	Part/kg fuel
11/10/00	15:38	15:51	I-494 going S	3.1E+14	1.4E+14	2.2E+15	1.0E+15
11/10/00	15:51	16:39	I-494 going S Traffic Jam			2.8E+15	3.0E+15
11/10/00	16:39	16:48	I-494 going E	4.7E+14	4.4E+14	3.4E+15	3.1E+15
11/15/00	14:17	14:20	I-494 going S	1.3E+15	3.5E+14	9.3E+15	2.5E+15
11/15/00	15:09	15:29	I-494 going S	1.6E+15	3.6E+14	1.1E+16	2.6E+15

As discussed previously, the SMPS provides estimates of the number, surface area and volume particle size distributions. The volume distribution is equivalent to the mass distribution if a particle density of 1 g/cm^3 is assumed (47-48). Data used to calculate mass fuel specific emissions are shown in table 4 and the estimates derived are shown in table 5. No estimate is shown for the period 14:17 to 14:20 on November 15 because the average background volume obtained from the SMPS continuous and bag samples was higher than the on-road volume estimate. This is in part due to the relative insensitivity of volume or mass estimates compared to number estimates.

Table 4. On-road data used for fuel specific and mg/mi mass emissions

Date	Time		Location	Speed mph	$CO + CO_2$ ppm		SMPS Cont μ^3/cm^3		SMPS Bag μ^3/cm^3	
	From	To		Mean	Mean	SD	Mean	SD	Mean	SD
11/10/00	14:46	15:00	Fernbrooke and 42nd	0	368	5	1.35	0.44	1.03	0.26
11/10/00	15:14	15:32	42nd Place	0	368	6	1.46	0.36	1.27	0.36
11/10/00	15:38	15:51	I-494 going S	46	421	47	3.97	3.11		
11/10/00	15:51	16:39	I-494 going S Traffic Jam	9	420	44	11.02	14.43		
11/10/00	16:39	16:48	I-494 going E	40	488	41	10.35	6.87		
11/15/00	14:17	14:20	I-494 going S	59	412	75	2.62	0.28		
11/15/00	14:24	14:39	Fernbrooke and 42nd	0	362	7	3.68	1.01	4.18	1.03
11/15/00	14:51	15:08	42nd Place	0	363	12	3.30	0.39	3.46	0.57
11/15/00	15:09	15:29	I-494 going S	44	415	55	5.78	1.82		

Table 5. On-road fuel specific particulate and mg/mi estimates derived from the SMPS

Date	Time		Location	SMPS	SMPS
	From	To		mg/mi	mg/kg fuel
11/10/00	15:38	15:51	I-494 going S	12.5	89
11/10/00	15:51	16:39	I-494 going S Traffic Jam		325
11/10/00	16:39	16:48	I-494 going E	18.6	132
11/15/00	14:17	14:20	I-494 going S		
11/15/00	15:09	15:29	I-494 going S	10.0	71

The particle/mi estimates shown in table 3 are higher for the CPC than for the SMPS. This may be due in part because of the greater sensitivity of the CPC to particles < 8 nm. Note that the size distributions shown in figures 53 and 54 for the specific periods of interest show that the particles measured on November 10th were, in general, larger than those measured on November 15th, and that the agreement between the two instruments is better on the 10th than the 15th. More data must be collected to confirm these results.

Our data are not dissimilar from data reported in other technical literature. In a European study (18) that evaluated diesel and spark ignition emissions in the laboratory, it was reported that at 50 km/h (31 mi/h) emissions from diesel vehicles varied considerably with the lowest emitting vehicle producing less than half the particle emissions of the highest emitting vehicle (8.0E13 compared to 2.0E14 particles/mi) while spark ignition vehicles produced much less. However, at high speed (120km/h or 75 mi/h), the pattern was different and both types of vehicles emitted large quantities of particles (1.9E14 to 2.9E14 particles/mi). Our concentrations tend to be higher for the following reasons.

- Cold weather favors nanoparticle formation.
- The SMPS was operated on the 8 to 300 nm range to maximize the opportunity to sample nanoparticles.

- The dilution conditions were representative of real world conditions that may favor nanoparticle formation. These conditions are not the same as those found in the typical laboratory dilution tunnel that may suppress nanoparticle formation.

In another study published by the Swedish National Road Administration (49) a variety of light duty compression (diesel) and spark ignition (gasoline) cars were evaluated on a chassis dynamometer. Particle/mi emissions for gasoline-fueled vehicles ranged from 1E12 to 1E14 for a moderate driving cycle and were higher by less than 1E15 for diesel vehicles. In this study the ELPI was used to determine the particle size distribution. Since the ELPI has a lower particle size cutpoint of 30 nm, it is likely that the estimates derived are low because particles < 30 nm would not have been counted.

CHAPTER 5
SUMMARY

The objective of this project was to obtain size distribution and number concentration data to characterize Minnesota roadway aerosol with an emphasis on nanoparticles. Rather than focusing on collecting data at ramps, data were collected on-road under varying traffic conditions and in residential areas different distances from the highway. When sampling in residential areas, data were collected upwind and downwind from the highway to determine the impact of the highway on residential air quality and to determine the effects of aerosol aging on the plume aerosol concentration and size distribution. On-road size distributions and fuel specific emissions were obtained.

Nearly all data were collected during cold weather, which is a limiting factor if the results are to be used to project particle number concentrations during summer months in Minnesota. Findings from studies conducted in our laboratory (50) have shown that the formation of nanoparticles is greatly enhanced by cold temperatures, thus additional data must be collected during warmer periods.

The primary instruments used in the study to characterize on-road particulate matter emissions were the SMPS, CPC, and the ELPI. In addition three gas analyzers, CO, CO_2, NO_X were used to characterize gaseous emissions on the highway.

Particulate matter emissions on-road ranged between 10^4 to 10^6 particles/cm^3, with the majority of the particles by number being less than 50 nm in diameter. An association between the on-road speed of the MEL and particle number concentration and particle size was observed: The higher the speed the greater the particle concentration and the smaller the particle size. This

is a reasonable finding because when the MEL was going 88 kmph (55 mph) the surrounding traffic was going 97 to 113 kmph (60 to 70 mph). At high vehicular speeds, particulate matter emissions increase because of increase engine load and fuel consumption. Passing diesel traffic was observed to further increase particle number concentrations. Measurements made in traffic jams with speeds < 32 kmph (20 mph) showed lower concentrations and larger particles. Some of the particles observed at higher speeds might have resulted from transient release of particle-associated materials stored in exhaust systems during lower speed operation. Others have observed this storage and release phenomenon (22). Less variation was observed in particle volume compared to particle number size distributions. Volume is probably influenced more by background concentrations than by local on-road conditions. Particle volume is a surrogate measure of particle mass and is conserved while particle number is constantly changing due to adsorption, agglomeration, coagulation and other physical and chemical mechanisms.

Measurements made in residential areas demonstrated that aerosol concentrations approached on-road concentrations when the residential area was 10-30 m (33-98 ft) from the highway and free from obstructions that could block the flow of air. The size distribution in these areas was similar to on-road aerosol with high concentrations of very small (<20 nm) particles. Much lower concentrations and much larger particles were observed in residential areas located 500 to 700 m (0.3 to 0.4 mi) from the highway.

Fuel specific and particle/mi emission rates were estimated from data collected on two different days. The particle/mi emissions were about an order of magnitude greater than published figures based upon results from laboratory studies. However, colder temperatures, different dilution and sampling conditions and different instrumentation could explain our increased estimates. More data needs to be collected to improve and validate these estimates.

The data collected during this study represent a unique database that will provide information on on-road emissions under cold climatic conditions. Further studies need to be completed to provide a more complete set of data, especially under warmer climatic conditions.

REFERENCES

1. Dockery, D.W., A. Pope III, X. Xu, J.D. Spengler, J.H. Ware, M.E. Fay, B.G. Ferris, Jr. and F.E. Speizer. "An Association Between Air Pollution and Mortality in Six U.S. Cities," New Eng. J. Med., Vol. 329, No. 24, pp. 1753-1759, 1993.

2. Pope III, C.A., M.J. Thun, M.M. Namboodiri, D.W. Dockery, J.S. Evans, F.E. Speizer and C.W. Heath, Jr. "Particulate Air Pollution as a Predictor of Mortality in a Prospective Study of U.S. Adults," Am. J. Respir. Crit. Care Med., Vol. 151, pp. 669-674, 1995.

3. Seaton, A., W. MacNee, K. Donaldson and D. Godden. "Particulate Air Pollution and Acute Health Effects: 1995," Lancet, Vol. 345, pp. 177, 1995.

4. Samet, J. M., F. Dominici, S. L. Zeger, J. Schwartz and D. W. Dockery. "The National Morbidity, Mortality, and Air Pollution Study Part I: Methods and Methodologic Issues," Health Effects Institute Report No 94, Part 1, 2000.

5. Samet, J. M., S. L. Zeger, F. Dominici, F. Curriero, I. Coursac, D. W. Dockery, J. Schwartz and A. Zanobetti. "The National Morbidity, Mortality,and Air Pollution Study. Part II: Morbidity, Mortality, and Air Pollution in the United States," Health Effects Institute Report No 94, Part 2, 2000.

6. Lippmann, M., K. Ito, A. Nádas and R. T. Burnett. "Association of Particulate Matter Components with Daily Mortality and Morbidity in Urban Populations," Health Effects Institute Report No. 95, 2000.

7. Oberdörster, G., J. N. Finkelstein, C. Johnston, R. Gelein, C. Cox, R. Baggs and A. C. P. Elder. "Acute Pulmonary Effects of Ultrafine Particles in Rats and Mice," Health Effects Institute Report No. 96, 2000.

8. Wichmann, H-E., C. Spix, T. Tuch, G. Wölke, A. Peters, J. Heinrich, W. G. Kreyling andJ. Heyder. "Daily Mortality and Fine and Ultrafine Particles in Erfurt, Germany. Part 1: Role of Particle Number and Particle Mass," Health Effects Institute Report No. 98, 2000.

9. Whitby, K. T. and B. K. Cantrell. "Atmospheric Aerosols - Characteristics and Measurement," ICESA Conference Proceedings, IEEE #75-CH 1004-1 ICESA, paper 29-1, 6 pp, 1975.

10. Bates, D. B., B. R. Fish, T. F. Hatch and T. T. Mercer and P. E. Morrow. "Deposition and Retention Models for Internal Dosimetry of the Human Respiratory Tract (Report of the international Commission on Radiological Protection: ICRP: Task Group on Lung Dynamics)," Health Phys. Vol. 12, No. 2. , pp. 173-207, 1966.

11. Raabe, O. G. "Deposition and Clearance of Inhaled Aerosols," Mechanism in Respiratory Toxicology, Vol. 1, pp. 27-76. H. Witschi and P. Nettesheim, Eds. CRC Press, Boca Raton, FL, 1982.

12. McCawley, M. A. "Should Dust Samples Mimic Human Lung Deposition? Counterpoint," Appl. Occup. Environ. Hyg. Vol. 5, No. 12, pp. 829-835, 1990.

13. Johnson, J. H. and K. J. Baumgard. "The Effect of Fuel and Engine Design on Diesel Exhaust Particle Size Distributions," Society of Automotive Engineers Tech. Pap. Ser. No. 960131, 1996.

14. The Airborne Particle Expert Group. "Source Apportionment of Airborne Particulate Matter in the United Kingdom," Report of the Airborne Particles Group, R Harrison, Chairman, available from http://www.environment.detr.gov.uk/airq/, 1999, 158 pp.

15. McAughey, J. J. "Regional Lung Deposition and Dose of Ambient Particulate in Humans by Particle Mass and Number," Research Report, AEA Technology, Aerosol Science Centre,

Oxfordshire, UK, 1997.

16. Booker, D. R. "Urban Pollution Monitoring: Oxford City Centre," Research Report, AEA Technology, Aerosol Science Centre, Oxfordshire, UK, 1997.

17. Hildemann, L. M., G. R. Markowski, M. C. Jones and G. R. Cass. "Submicrometer Aerosol Mass Distributions of Emissions from Boilers, Fireplaces, Automobiles, Diesel Trucks, and Meat-Cooking Operations," Aerosol Sci. Technol., Vol. 14, pp. 138-152, 1991.

18. Rickeard, D. J., J. R. Bateman, Y. K. Kwon, J. J. McAughey and C. J. Dickens. "Exhaust Particulate Size Distribution: Vehicle and Fuel Influences in Light Duty Vehicles". Society of Automotive Engineers Tech. Pap. Ser. No. 961980, 1996.

19. Maricq, M. M., D. H. Podsiadlik and R. E. Chase. "Examination of the Size-Resolved and Transient Nature of Motor Vehicle Particle Emissions," Environ. Sci. Technol. Vol. 33, pp. 1618-1626, 1999.

20. Maricq, M. M., D. H. Podsiadlik and R. E. Chase. "Gasoline Vehicle Particle Size Distributions: Comparison of Steady State, FTP, and USO6 Measurements," Environ. Sci. Technol. Vol. 33, pp. 2007-2015, 1999.

21. Hall, D. E. and C. J. Dickens. "Measurement of the Number and Size Distribution of Particles Emitted from a Gasoline Direct Injection Vehicle," Society of Automotive Engineers Tech. Pap. Ser. No. 1999-01-3530, 11 pp., 1999.

22. Hall, D. E. and C. J. Dickens. "Measurement of the Numbers of Emitted Gasoline Particles: Genuine or Artifact?" Society of Automotive Engineers Tech. Pap. Ser. No.2000-01-2957, 9 pp., 2000.

23. Abdul-Khalek, I. S. and. D. B. Kittelson. "Real Time Measurement of Volatile and Solid Exhaust Particles Using a Catalytic Stripper," Society of Automotive Engineers Tech. Pap. Ser.

No. 950236, 1995.

24. Cadle, S. H. and P. A. Mulawa. "Particulate Emission Rates from In-Use High-Emitting Vehicles Recruited in Orange County, California," Env. Sci. Tech., Vol. 31, pp. 3405-3412, 1997.

25. Graskow, B. R., D.B. Kittelson, I. S. Abdul-Khalek, M. R. Ahmadi and J.E. Morris. "Characterization of Exhaust Particulate Emissions from a Spark Ignition Engine," Society of Automotive Engineers Tech. Pap. Ser. No. 980528, 10 pp, 1998.

26. Bagley, S. T., K. J. Baumgard, L. D. Gratz, J. J. Johnson and D. G. Leddy. "Effects of Fuel Modification and Emission Control Devices on Heavy-Duty Diesel Engine Emissions," Health Effects Institute (HEI), Research Report No. 76., 1996.

27. Dolan, D. F., D. B. Kittelson and D. Y. H. Pui. Diesel Exhaust Particle Size Distribution Measurement Technique," Society of Automotive Engineers Tech. Pap. Ser. No. 800187, 1980.

28. Kittelson, D. B., P. A. Kadue, H. C. Scherrer and R. E. Lovrien. "Characterization of Diesel Particles in the Atmosphere," Final Report, Coordinating Research Council, 1988.

29. Baumgard, K. J. and D. B. Kittelson. "The Influence of a Ceramic Particle Trap on the Size Distribution of Diesel Particles," Society of Automotive Engineers Transactions, Vol. 95, pp. 56-69, 1985.

30. Abdul-Khalek, I. S., D. B. Kittelson, B. R. Graskow, Q. Wei and F. Brear. "Diesel Exhaust Particle Size: Measurement Issues and Trends," Society of Automotive Engineers Tech. Pap. Ser. No. 980525, 1998.

31. Abdul-Khalek, I., D.B. Kittelson and F. Brear. "The Influence of Dilution Conditions on Diesel Exhaust Particle Size Distribution Measurements," Society of Automotive Engineers Tech. Pap. Ser. No. 1999-01-1142, 1999.

32. Friedlander, S. K. Smoke, Dust and Haze: Fundamentals of Aerosol Behavior. New York, John Wiley and Sons, 1977.

33. Khalek, I. A., D. B. Kittelson and F. Brear. "Nanoparticle Growth During Dilution and Cooling of Diesel Exhaust: Experimental Investigation and Theoretical Assessment," Society of Automotive Engineers Tech. Pap. Ser. No. 2000-01-0514, 9 pp., 2000.

34. Jing, L., Bach, C. and Forss, A. "Einfluss des Einspritzdruckes auf die Partikelemission des DI-Dieselfahrzeuges," Zeitschrift fur das Messwesen Vol. 3, pp. 7-10, 1996.

35. Kruger, M., H. Lüders, B. Lüers, R. Kaufmann, W. Koch and T. Kauffeldt. "Influence of Exhaust Gas Aftertreatment on Particulate Characteristics of Vehicle Diesel Engines," Research Report of the Forschungsvereinigung Verbrennungskraftmaschinen e.V. (FVV). MTZ Motortechnische Zeitschrift Vol. 58, pp. 27-30, 1997.

36. Mayer, A., H. Egli, H. Burtscher, J. Czerwinski, D. Gehrig and H. T. L. Biel. "Particle Size Distribution Downstream Traps of Different Design," Society of Automotive Engineers Tech. Pap. Ser. No. 950373, 1995.

37. Mayer, A., U. Matter, G. Scheidegger, J. Czerwinski, M. Wyser, D. Kieser and J. Weidhofer. "Particulate Traps for Retro-Fitting Construction Site Engines VERT: Final Measurements and Implementation," Society of Automotive Engineers Tech. Pap. Ser. No. 1999-01-0116, 1999.

38. Ping, J. I., D. Mark and R. M. Harrison. "Characterization of Particles from a Current Technology Heavy-Duty Engine," Env. Sci. Technol. Vol. 34, No. 5, pp. 748-755, (2000).

39. Harrison, R. M. "Airborne Particulate Matter in the United Kingdom," Third Report of the Quality of Urban Air Review Group. Edgbaston, England, The University of Birmingham, 1996.

40. Cadle, S. H., P. Mulawa, E. C. Hunsanger, K. Nelson, R. A. Ragazzi, R. Barrett, G. L.

Gallagher, D. R. Lawson, K. T. Knapp and R. Snow. "Measurement of Exhaust Particulate Matter Emissions from In-Use Light-Duty Motor Vehicles in the Denver, Colorado Area," Coordinating Research Council Project E-24-1 Final Report, CRC, Atlanta, GA, 142 pp., 1998.

41. Watson, J. G., E. M. Fukita, J. C. Chow, B. Zielinska, I. W. Richards, W. Neff, and D. Dietrich. "Northern Front Range Air Quality Study Final Report," Document No. 6580-685-8750-IF2: Desert Research Institute, Reno, NC, 1998.

42. Schlichting, H. Boundary-Layer Theory. McGraw-Hill, New York, 817 pp. 1979.

43. Seinfeld, J. H. and S. N. Pandis. Atmospheric Chemistry and Physics. John Wiley and Sons, Inc., 1998, New York, NY. 1326 pp.

44. Heywood, J. B. Internal Combustion Engine Fundamentals. McGraw-Hill Book Co., New York, NY, 1988, 930 pp.

45. Chevron. "Motor Gasolines Technical Review," FTR-1 Chevron Products Company, 1996, 66 pp.

46. Owen, K. and T. Coley. Automotive Fuels Reference Book. Second Edition, Society of Automotive Engineers, Inc, Warrendale, PA, 963 pp.

47. Kittelson, D. B., D. F. Dolan, R. B. Diver and E. Aufderheide. "Diesel Exhaust Particle Size Distributions – Fuel and Additive Effects," Society of Automotive Engineers Tech. Pap. Ser. No. 780787, 1978, 12 pp.

48. Kittelson, D. B., P. A. Kadue, H. C. Scherrer and R. E. Lovrien. "Characterization of Diesel Particles in the Atmosphere," Coordinating Research Council AP-2 Project Group Final Report, CRC, Alpharetta, GA, 1988.

49. Färnlund, J., Homan, C. and Kågeson, P. "Emissions of Ulrafine Particles from Different Types of Light Duty Vehicles," Swedish National Road Administration Publication, 2001:10, 16

pp., 2001.

50. Wei, Q., D. B. Kittelson and W. F. Watts. "Single-Stage Dilution Tunnel Performance," Society of Automotive Engineers Tech. Pap. Ser. No. 2001-01-0201, 2001, 12 pp.

FIGURES

Figure 1. MEL chasing a truck on a rural Minnesota road

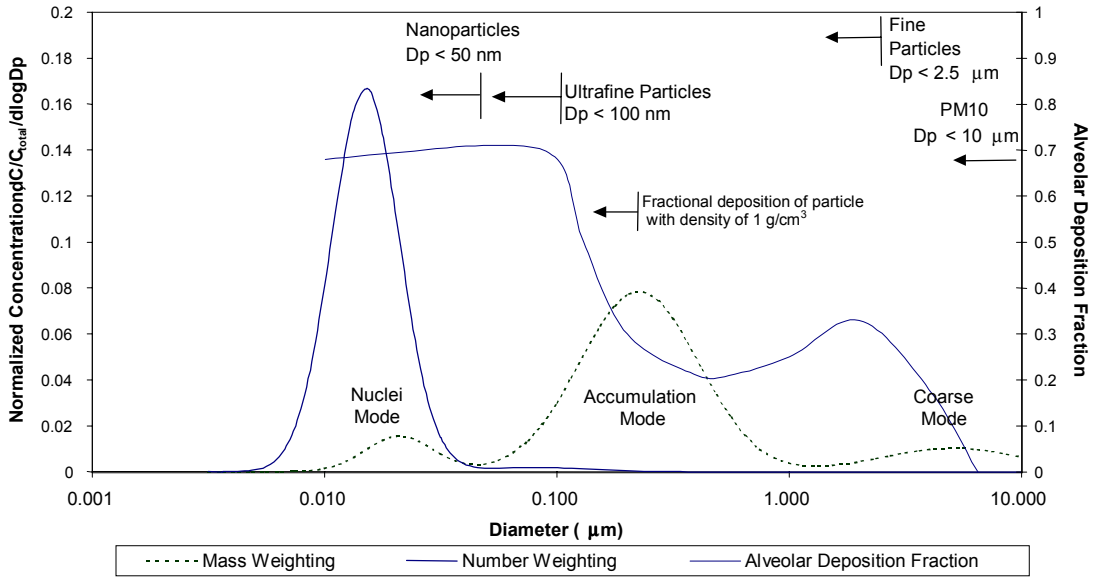

Figure 2. Typical diesel engine exhaust mass and number weighted size distributions shown with alveolar deposition

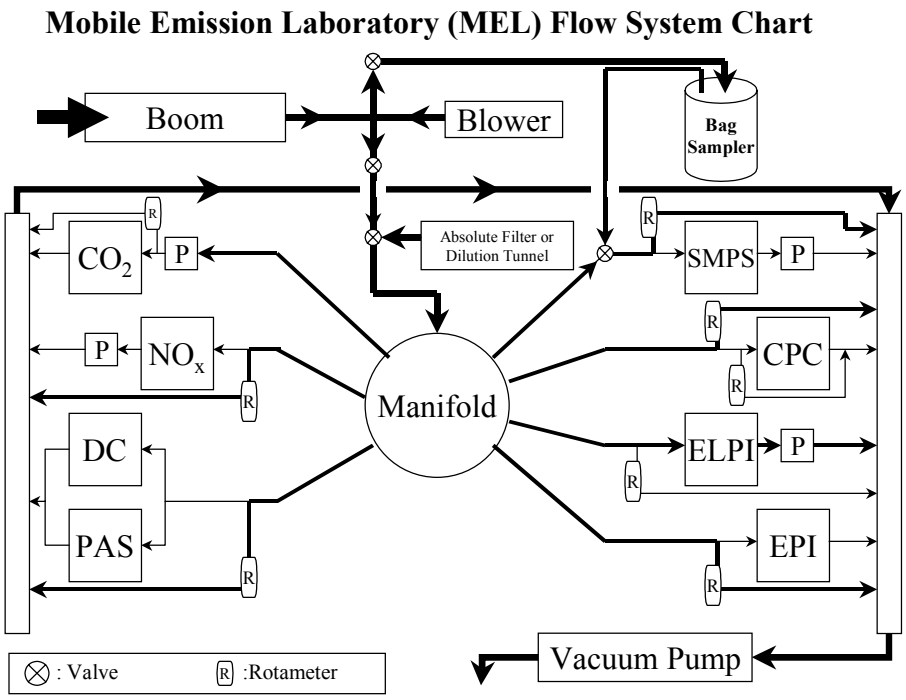

Figure 3. Schematic of MEL sampling system and instrumentation.
CO_2 carbon dioxide monitor, NOx oxides of nitrogen monitor, DC diffusion charger, PAS photoemission detector, SMPS scanning mobility particle sizer, CPC condensation particle counter, ELPI electrical low pressure impactor, EPI epiphaniometer, not shown carbon monoxide monitor, P pump.

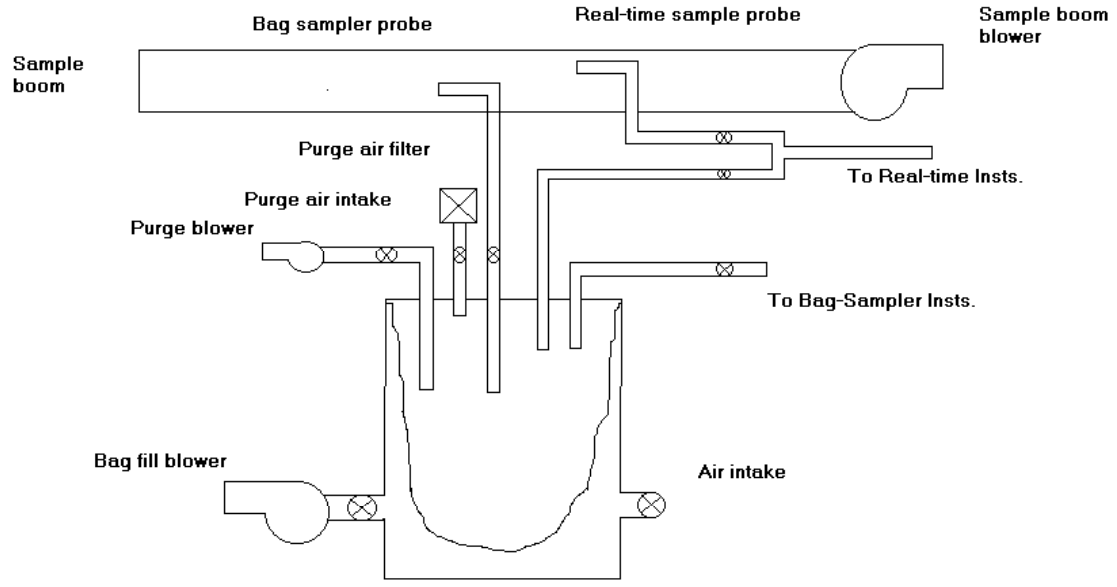

Figure 4. Schematic of the MEL bag sampler

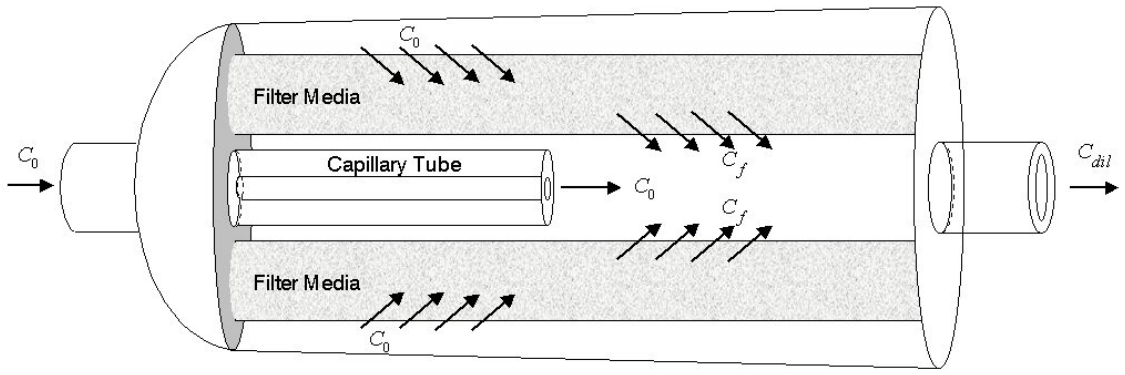

Figure 5. Schematic diagram of the leaky-filter dilutor

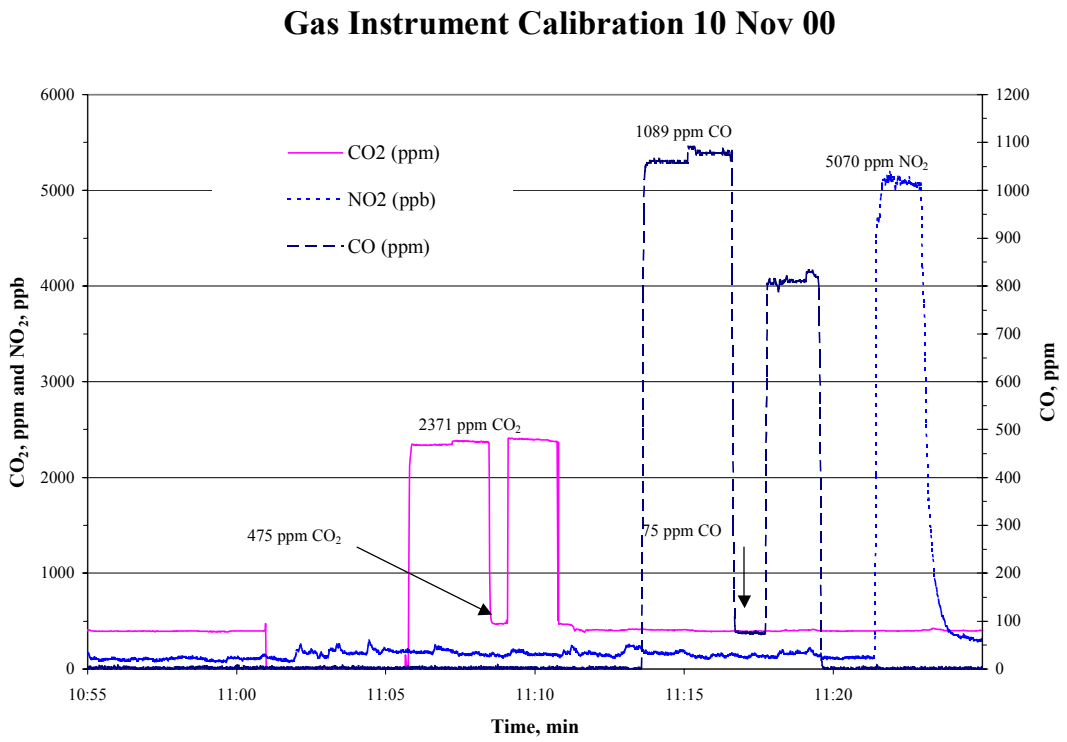

Figure 6. Gas instrument calibration on November 10, 2000

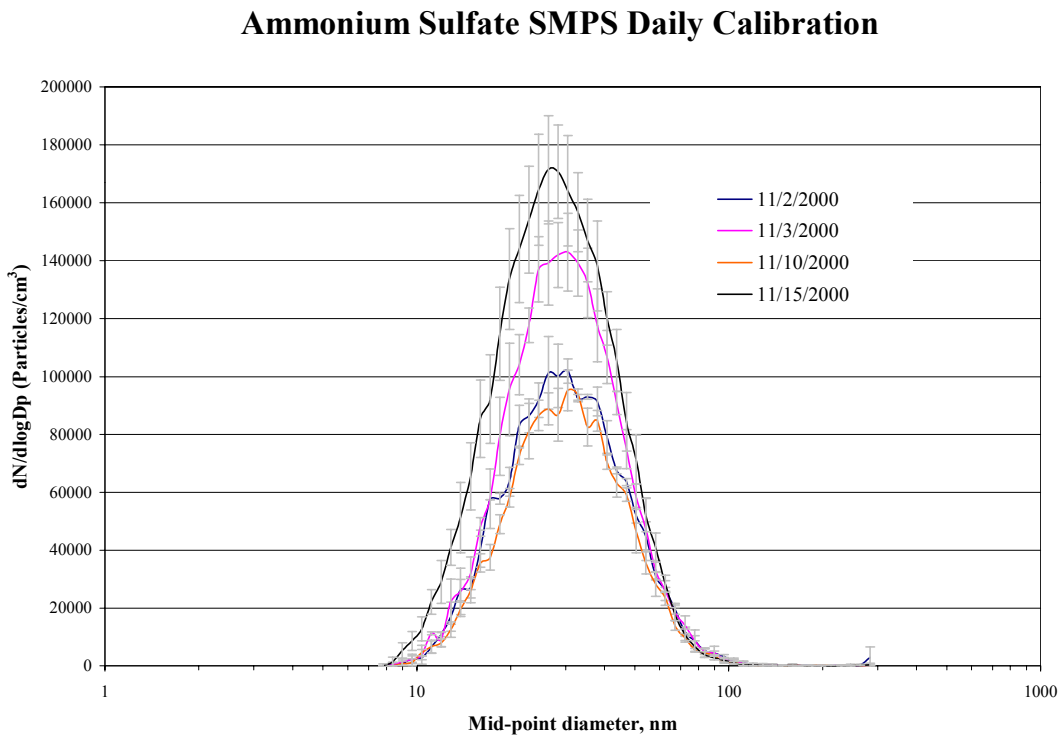

Figure 7. Ammonium sulfate daily consistency check of the SMPS

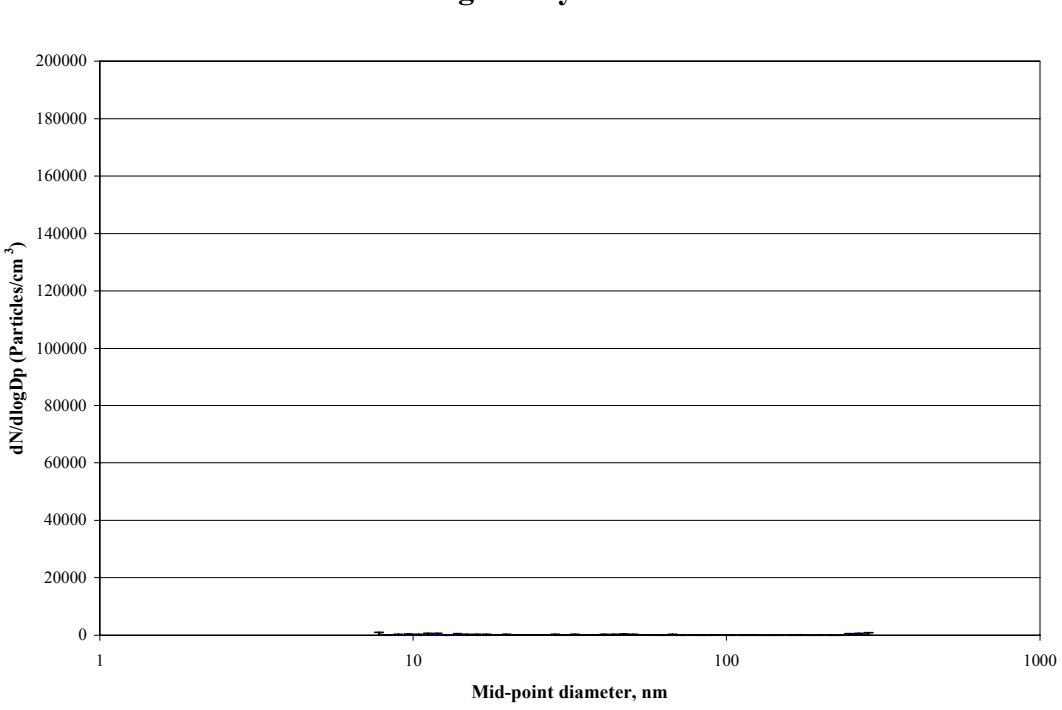

Figure 8. Daily average absolute filter results from the SMPS

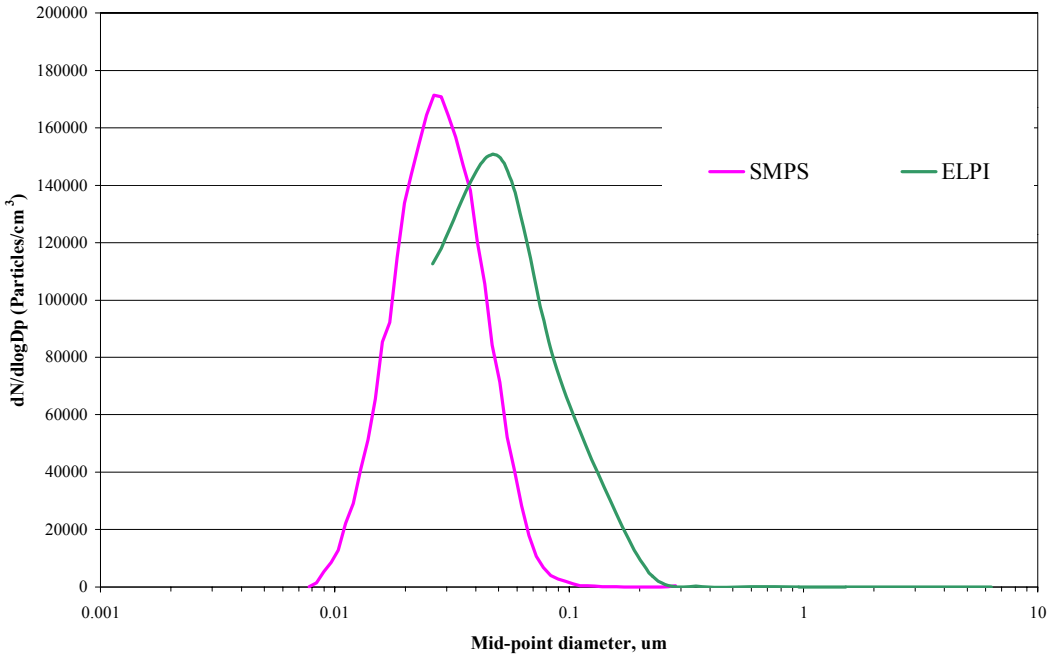

Figure 9. Ammonium sulfate calibration comparison of the SMPS and ELPI

Figure 10. Route map

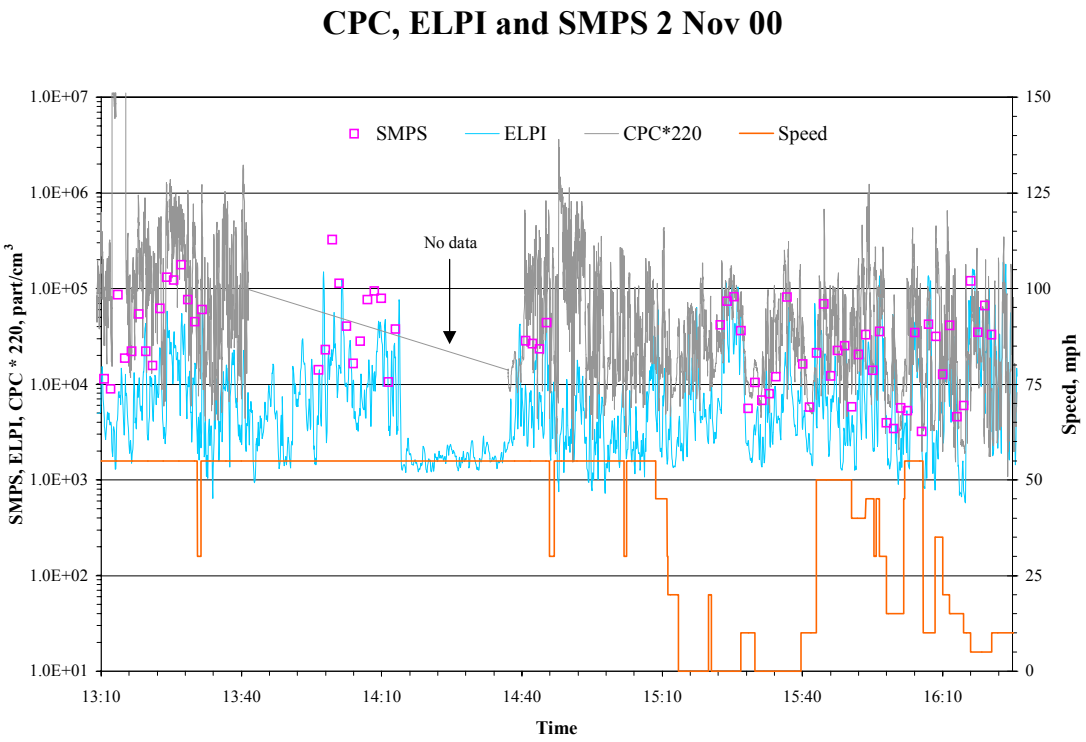

Figure 11. CPC, ELPI and SMPS 2 Nov 00

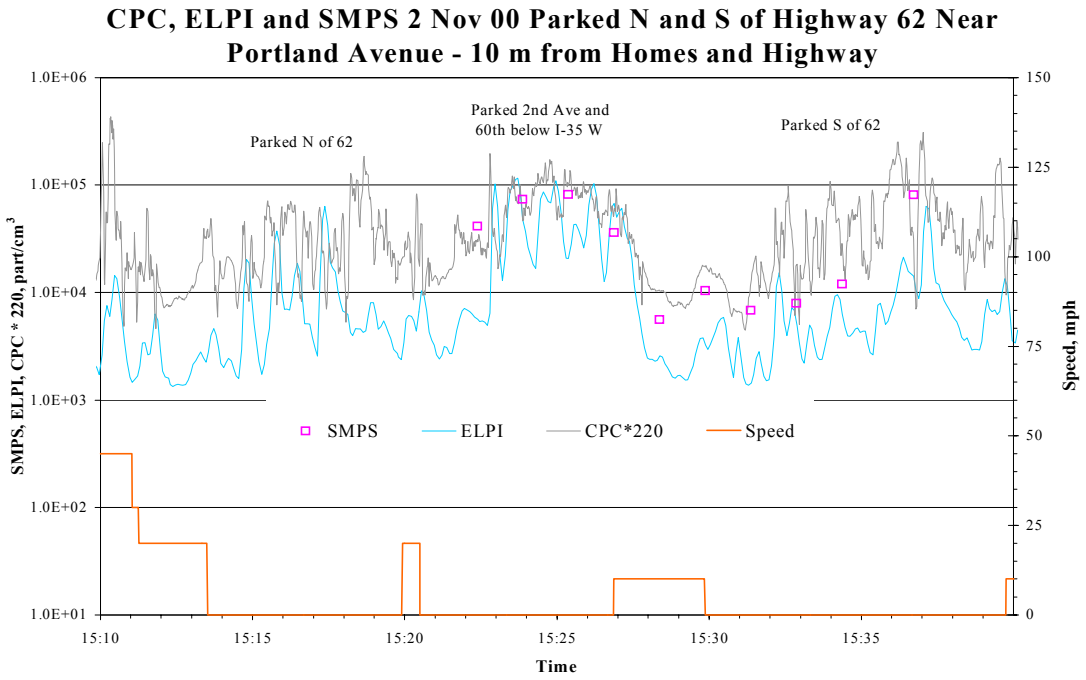

Figure 12. CPC, ELPI and SMPS 2 Nov 00 Parked N and S of Highway 62 Near Portland Avenue

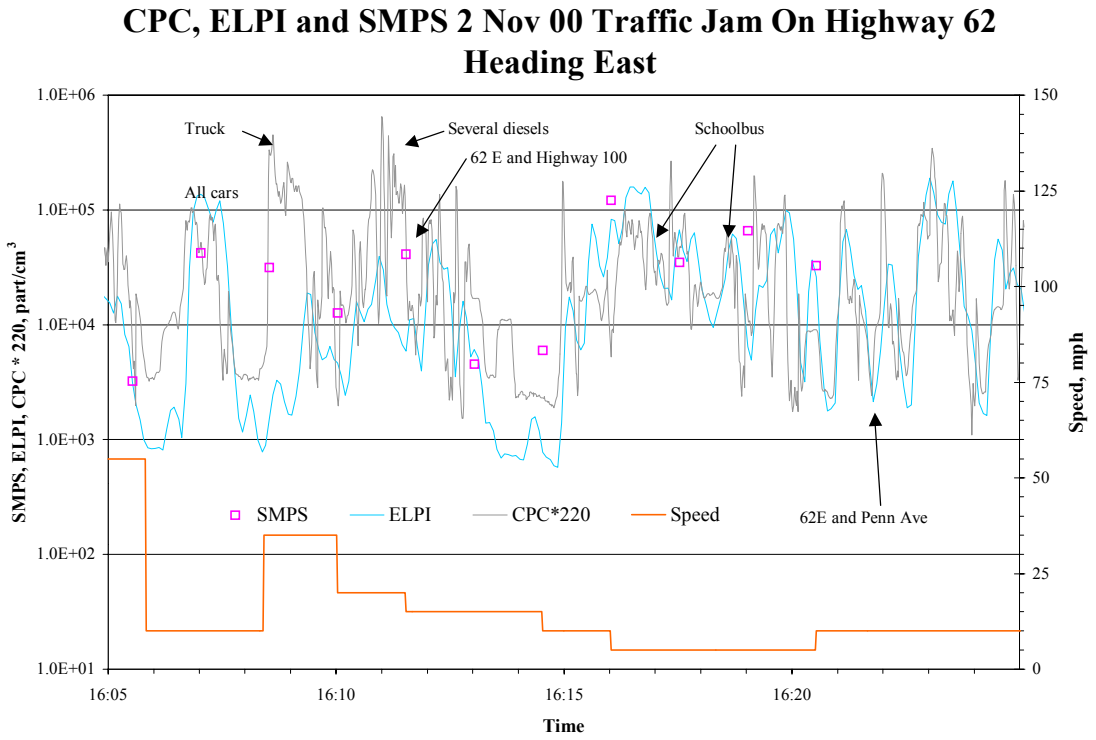

Figure 13. CPC, ELPI and SMPS 2 Nov 00 Traffic Jam on Highway 62 Heading East

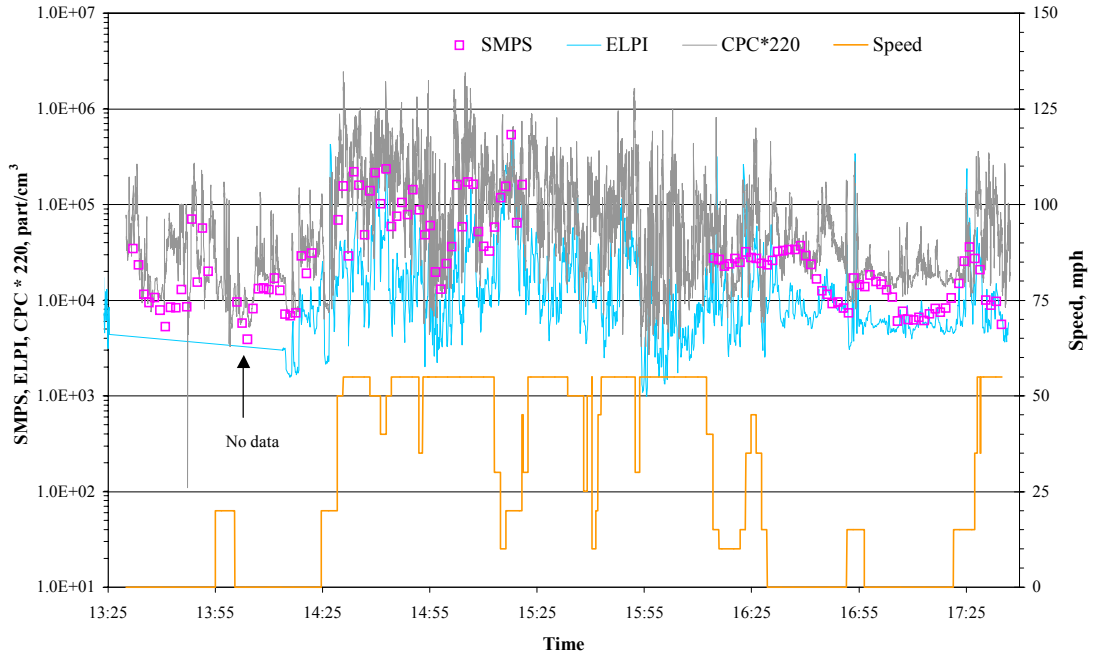

Figure 14. CPC, ELPI and SMPS 3 Nov 00

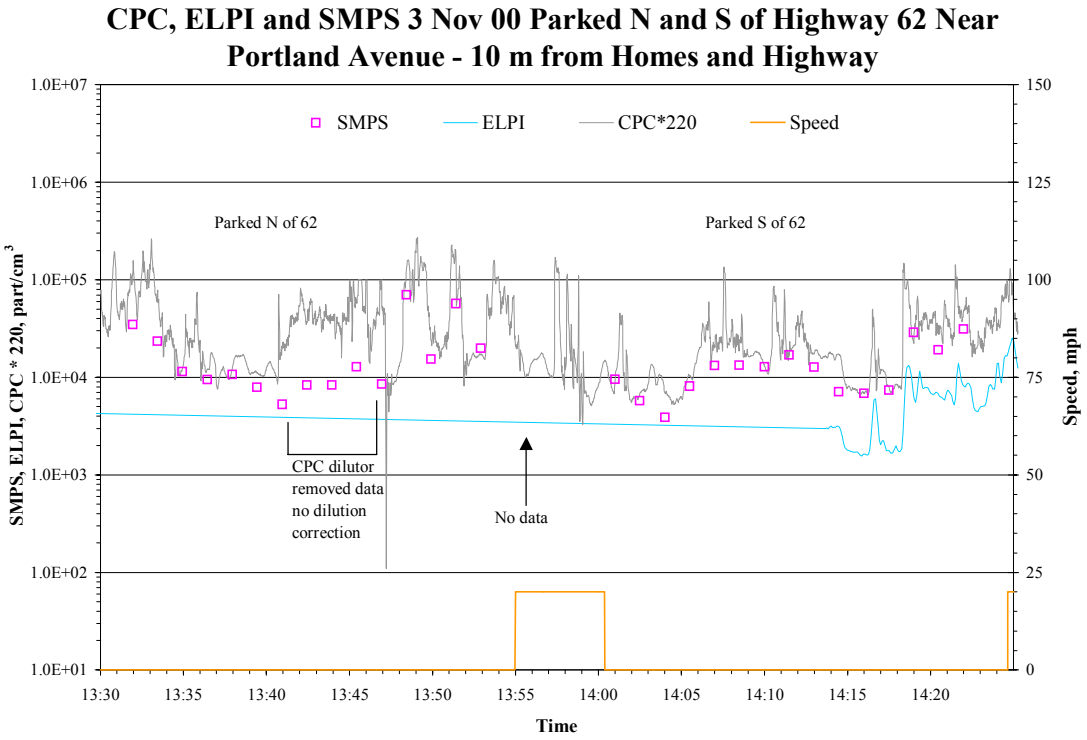

Figure 15. CPC, ELPI and SMPS 11/3/00 Parked N and S of Highway 62 Near Portland Ave.

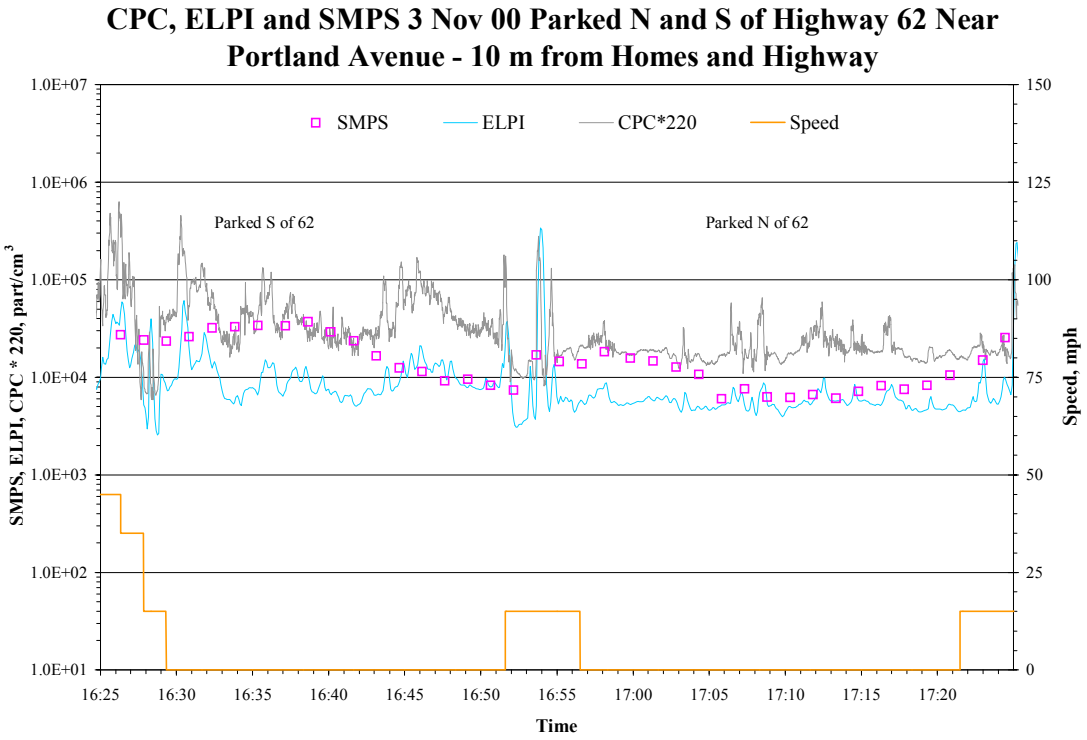

Figure 16. CPC, ELPI and SMPS 11/3/00 Parked N and S of Highway 62 Near Portland Ave.

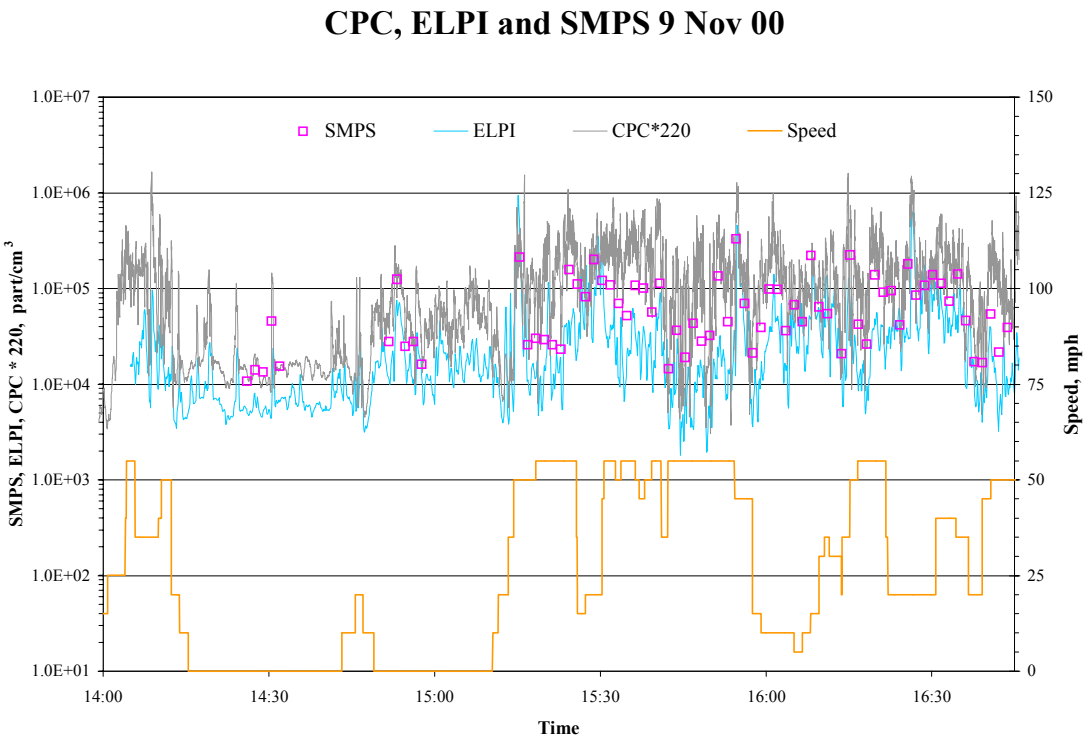

Figure 17. CPC, ELPI and SMPS 9 Nov 00

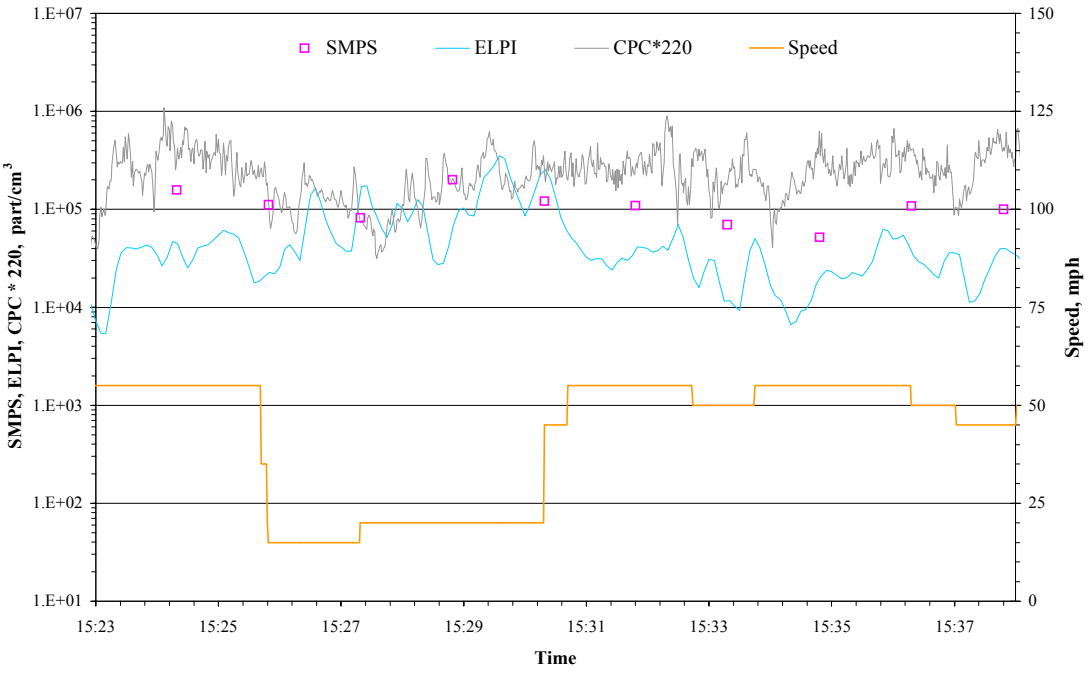

Figure 18. CPC, ELPI and SMPS 9 Nov 00 County Road 169 Various Speed

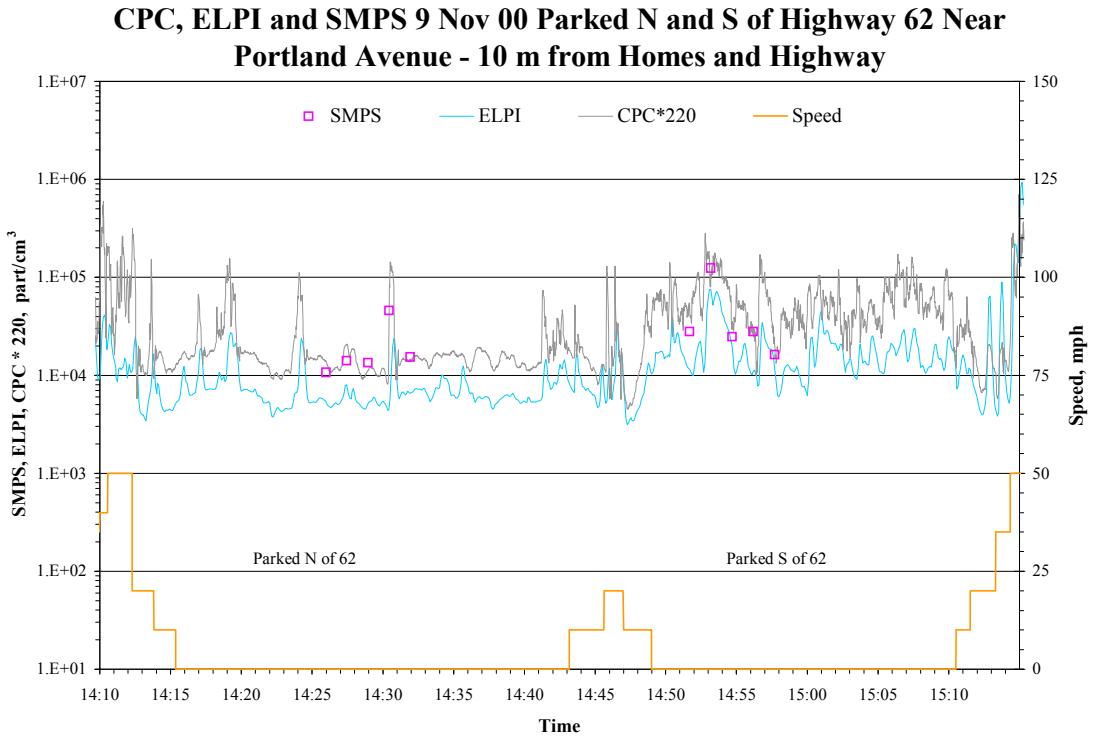

Figure 19. CPC, ELPI and SMPS 3/9/00 Parked N and S of Highway 62 Near Portland Ave.

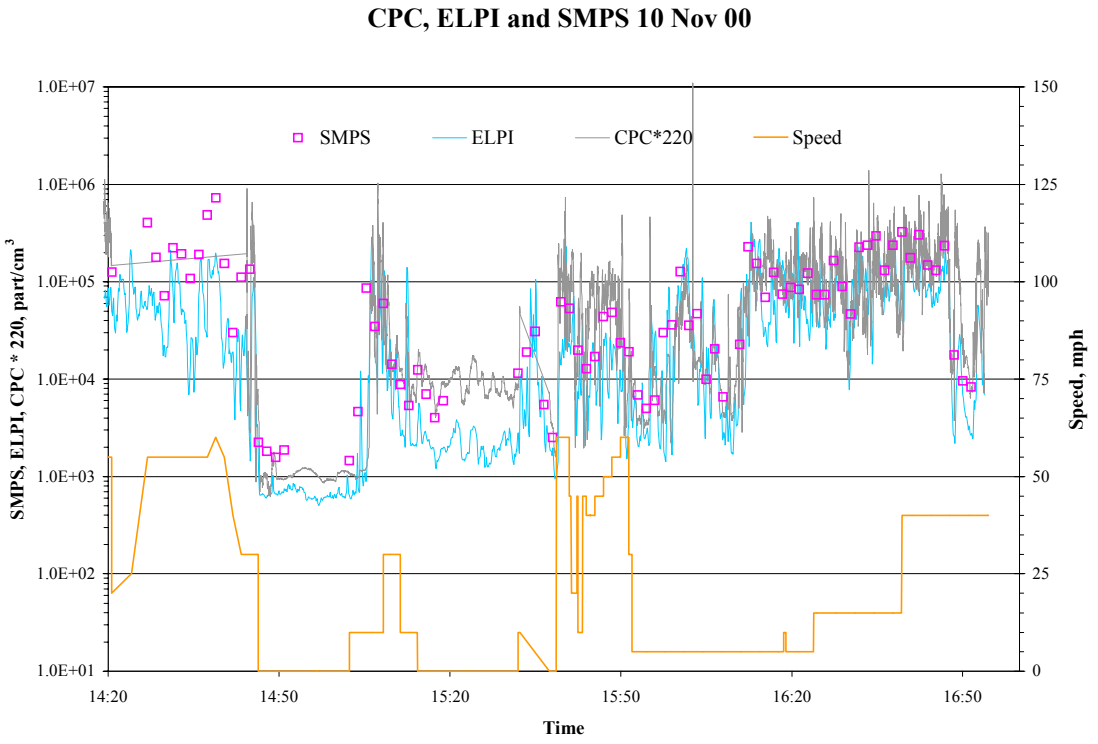

Figure 20. CPC, ELPI and SMPS 10 Nov 00

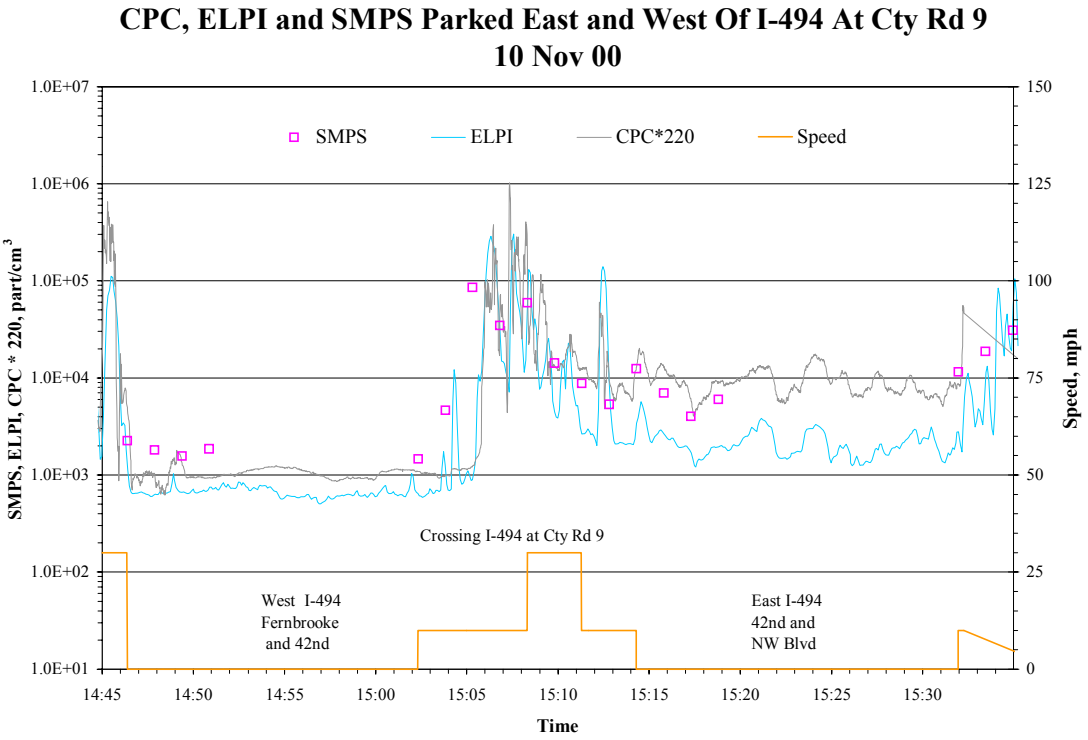

Figure 21. CPC, ELPI and SMPS Parked East and West of I-494 At Cty Rd 9 10 Nov 00

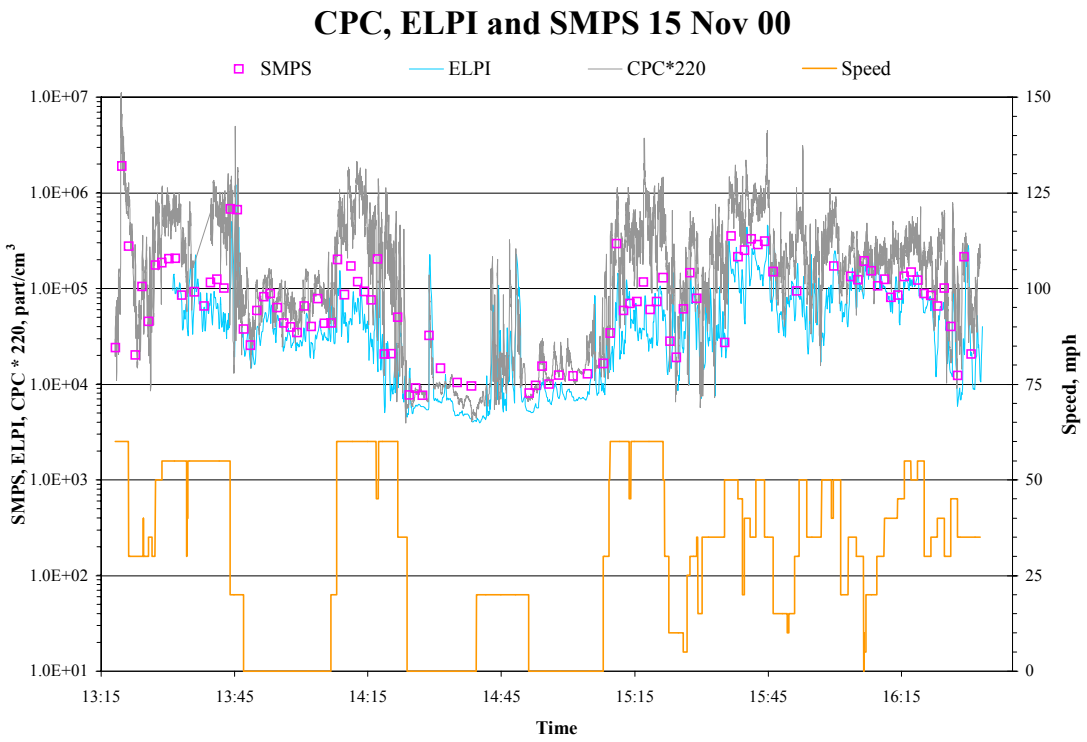

Figure 22. CPC, ELPI and SMPS 15 Nov 00

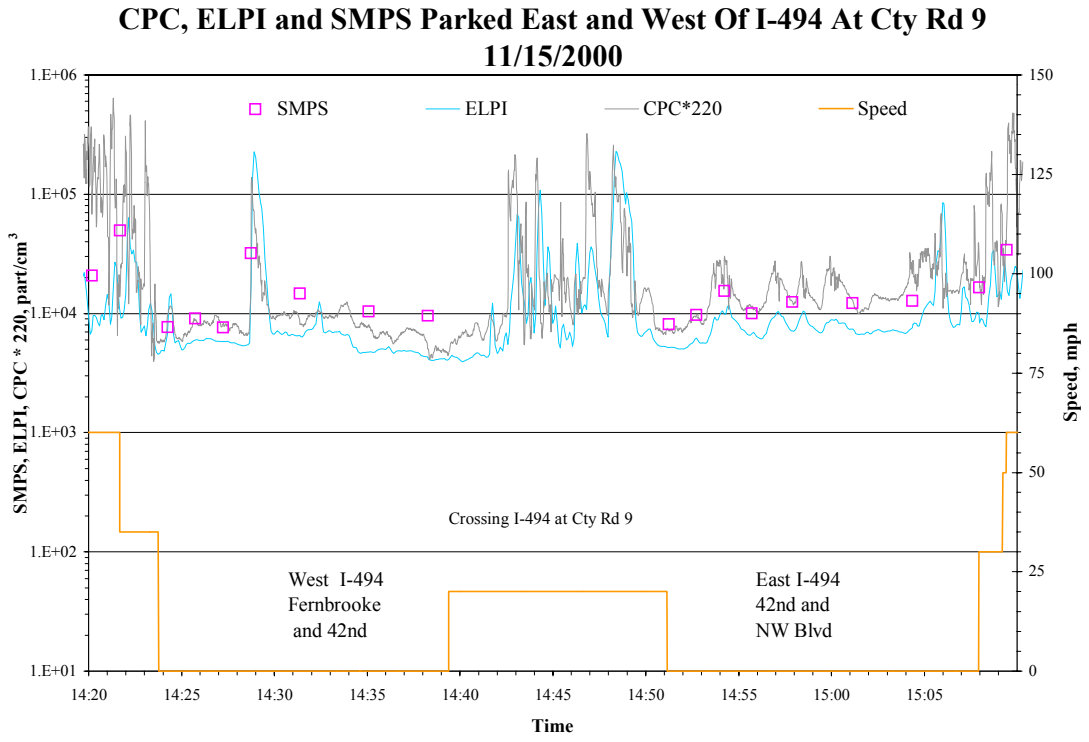

Figure 23. CPC, ELPI and SMPS Parked East and West of I-494 At Cty Rd 9 15 Nov 00

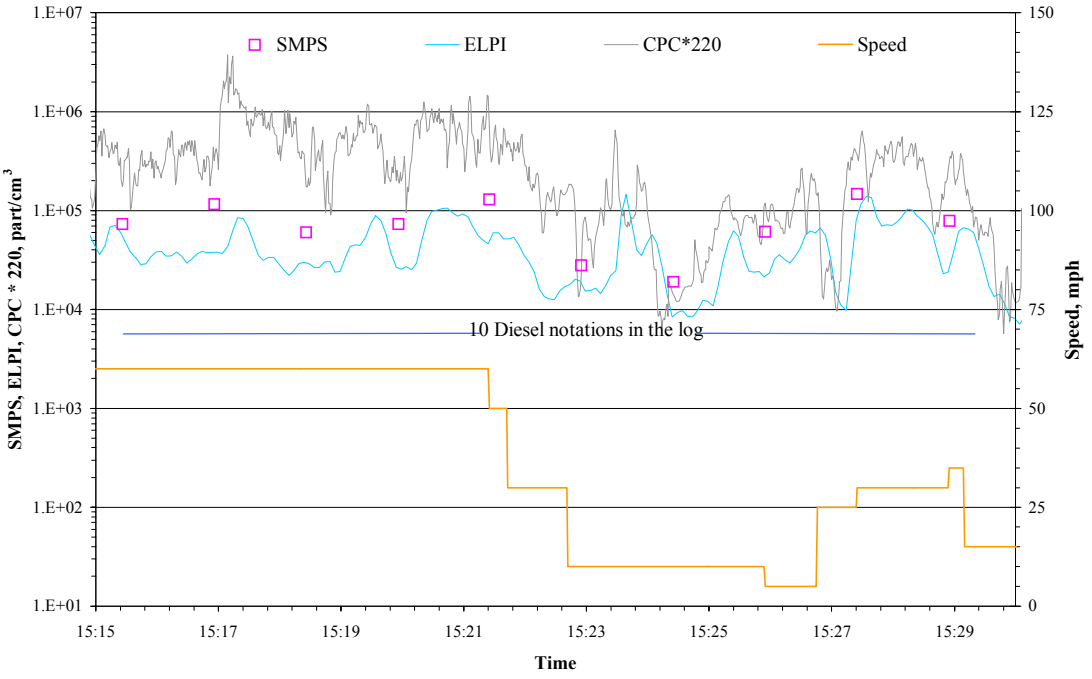

Figure 24. CPC, ELPI, SMPS 15 Nov 00 I-494 Various Speed

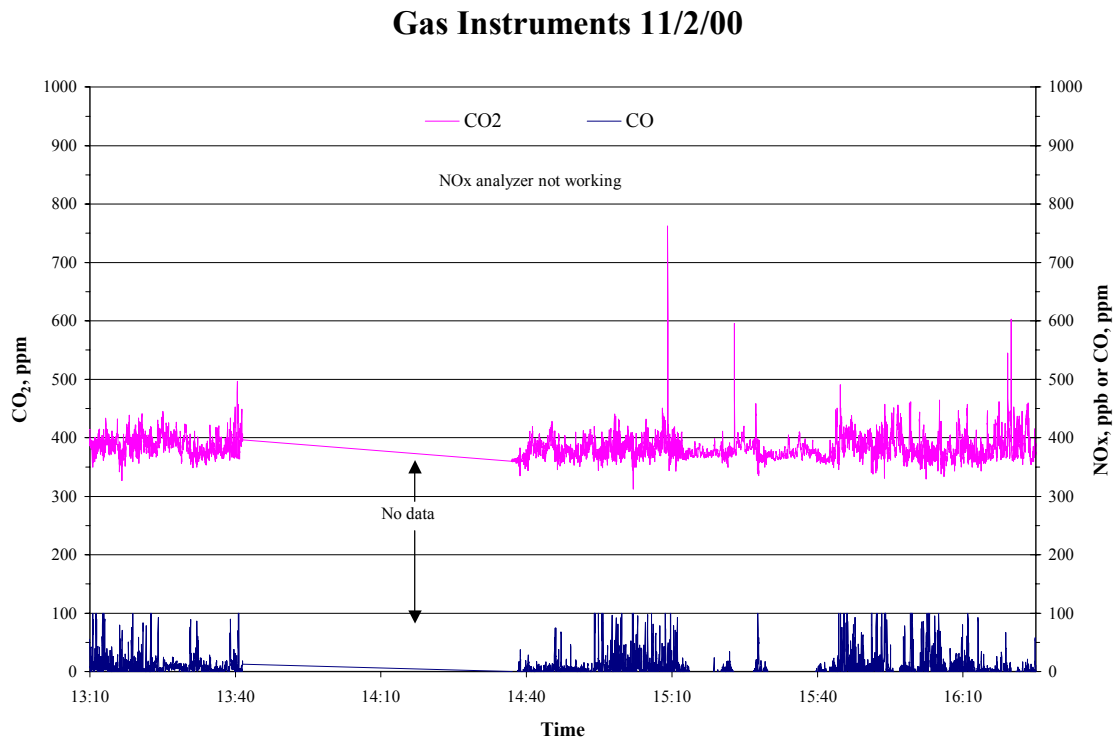

Figure 25. Gas Instruments 11/2/00

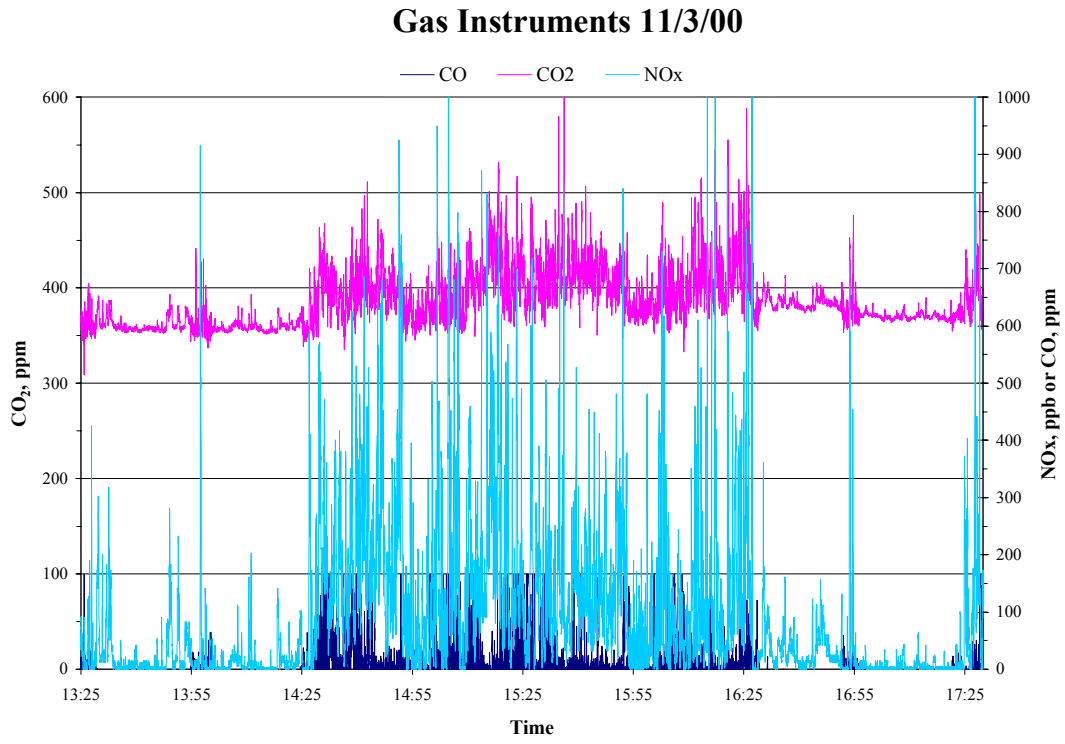

Figure 26. Gas Instruments 11/3/00

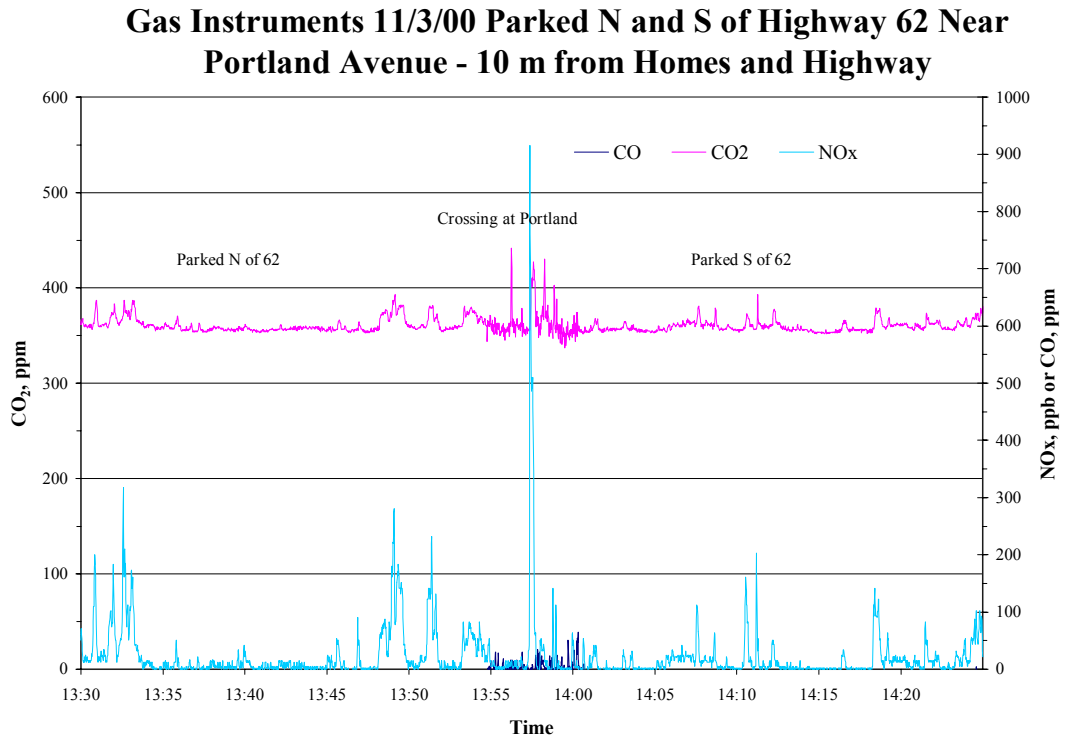

Figure 27. Gas Instruments 11/3/00 Parked N and S of Highway 62 Near Portland Avenue

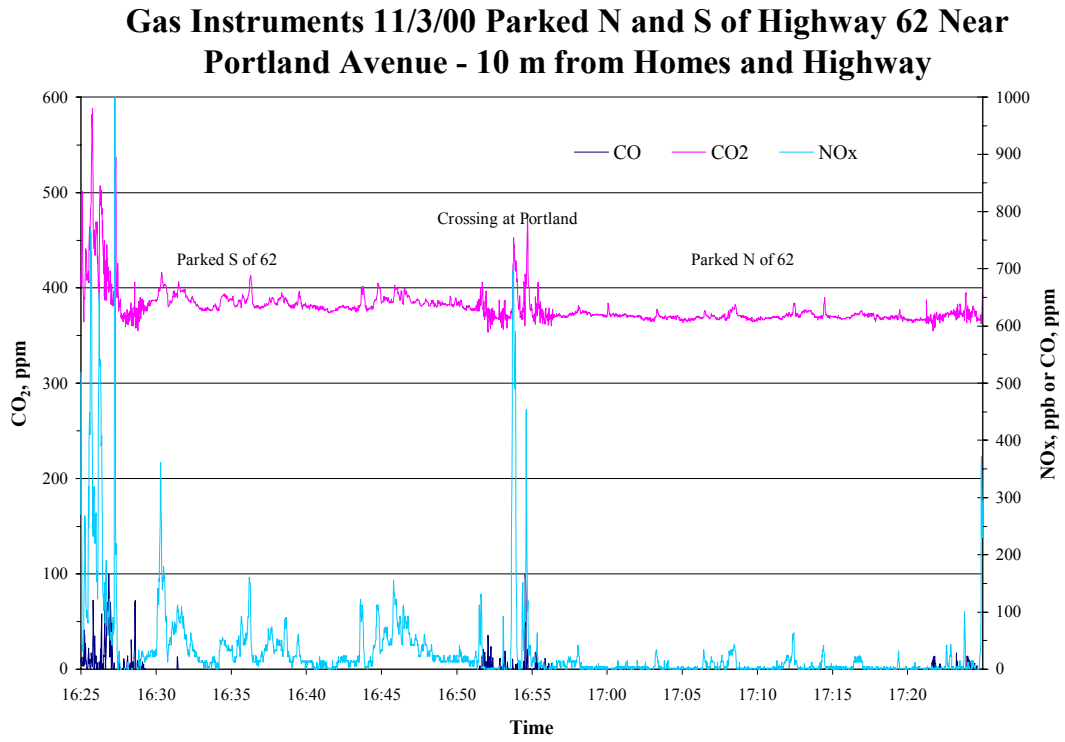

Figure 28. Gas Instruments 11/3/00 Parked N and S of Highway 62 Near Portland Avenue

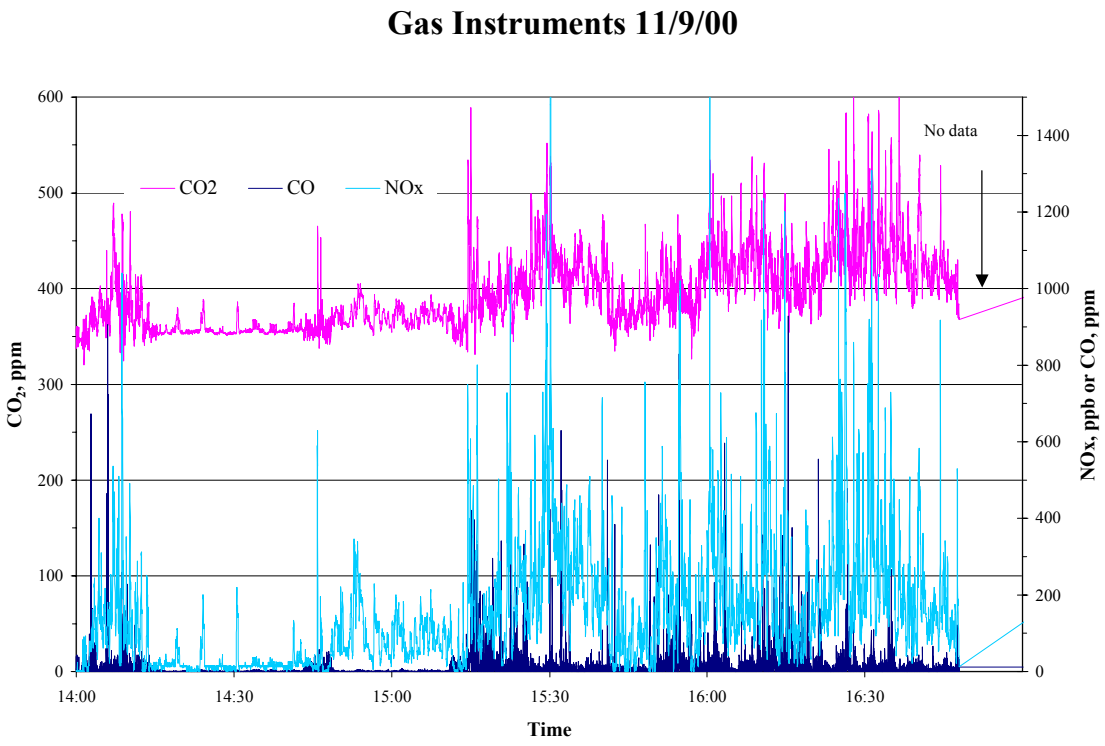

Figure 29. Gas Instruments 11/9/00

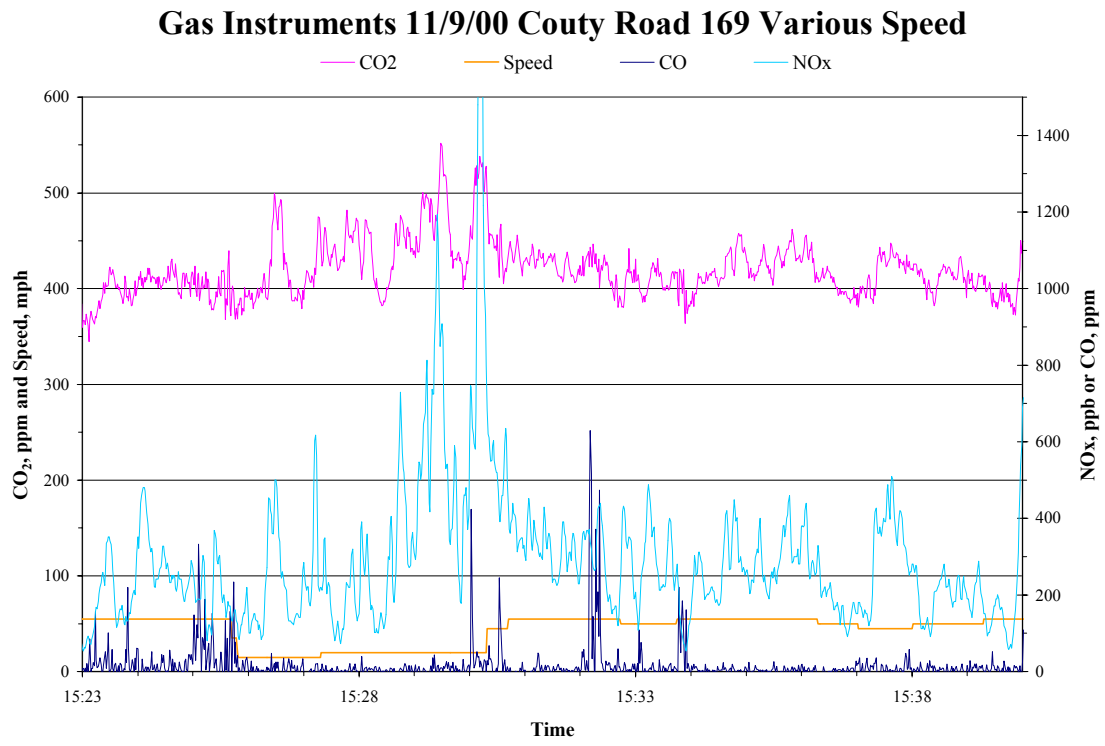

Figure 30. Gas Instruments 11/9/00 County Road 169 Various Speed

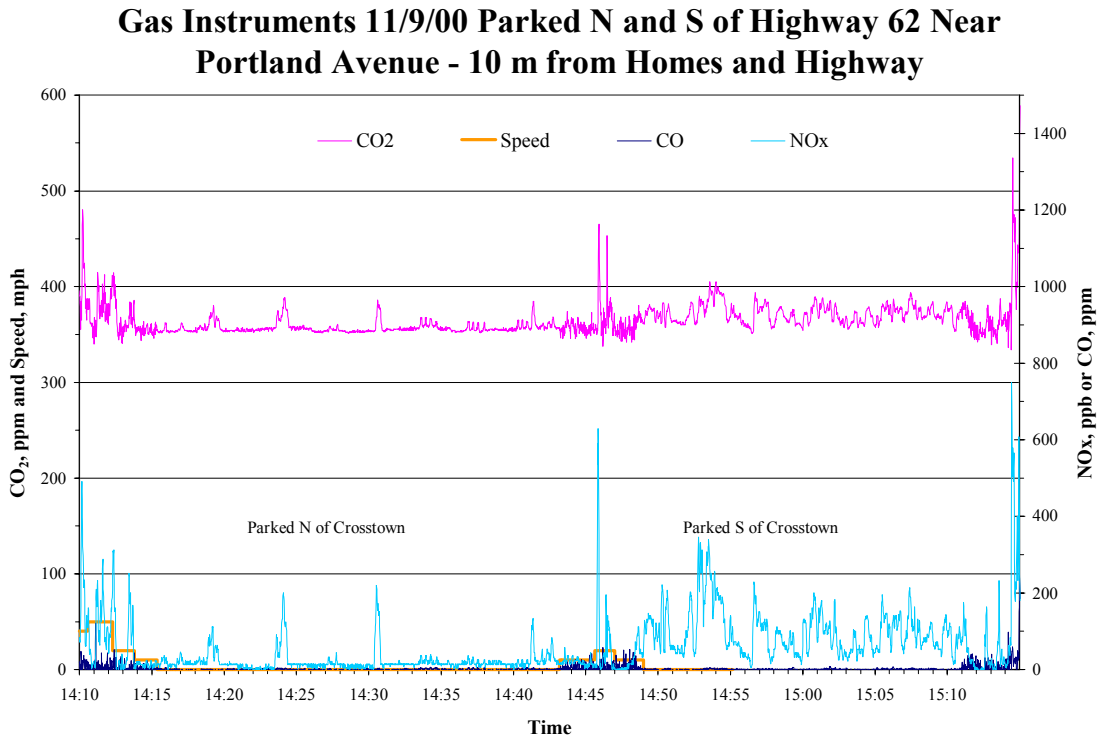

Figure 31. Gas Instruments 11/9/00 Parked N and S of Highway 62 Near Portland Avenue

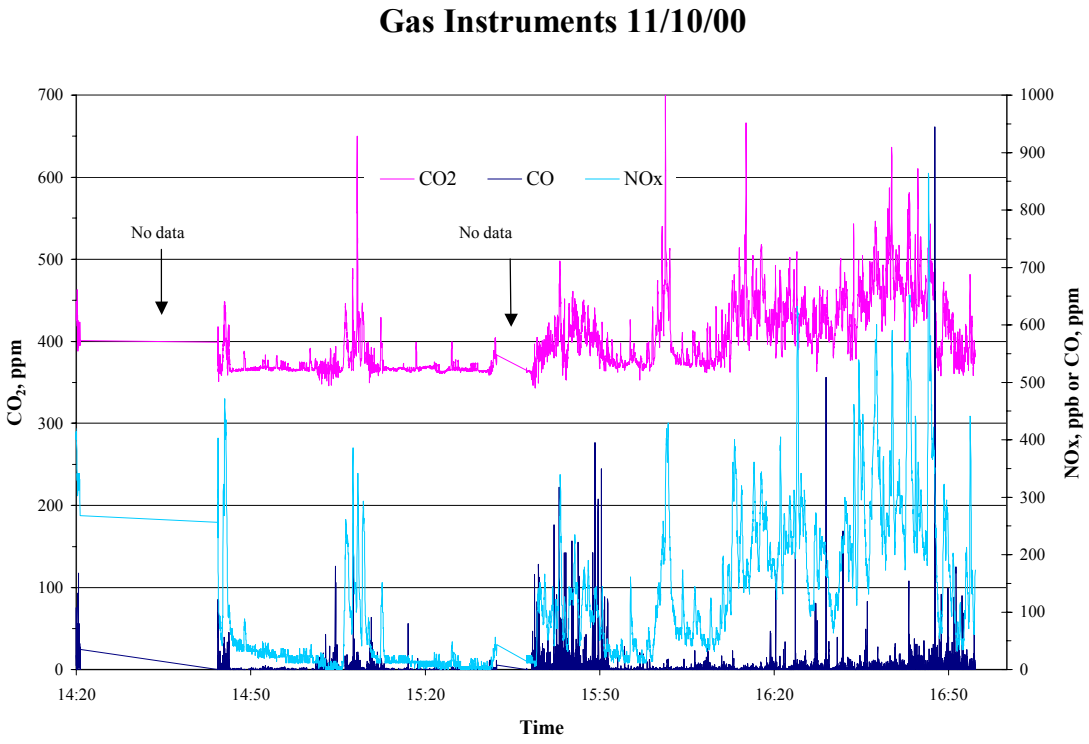

Figure 32. Gas Instruments 11/10/00

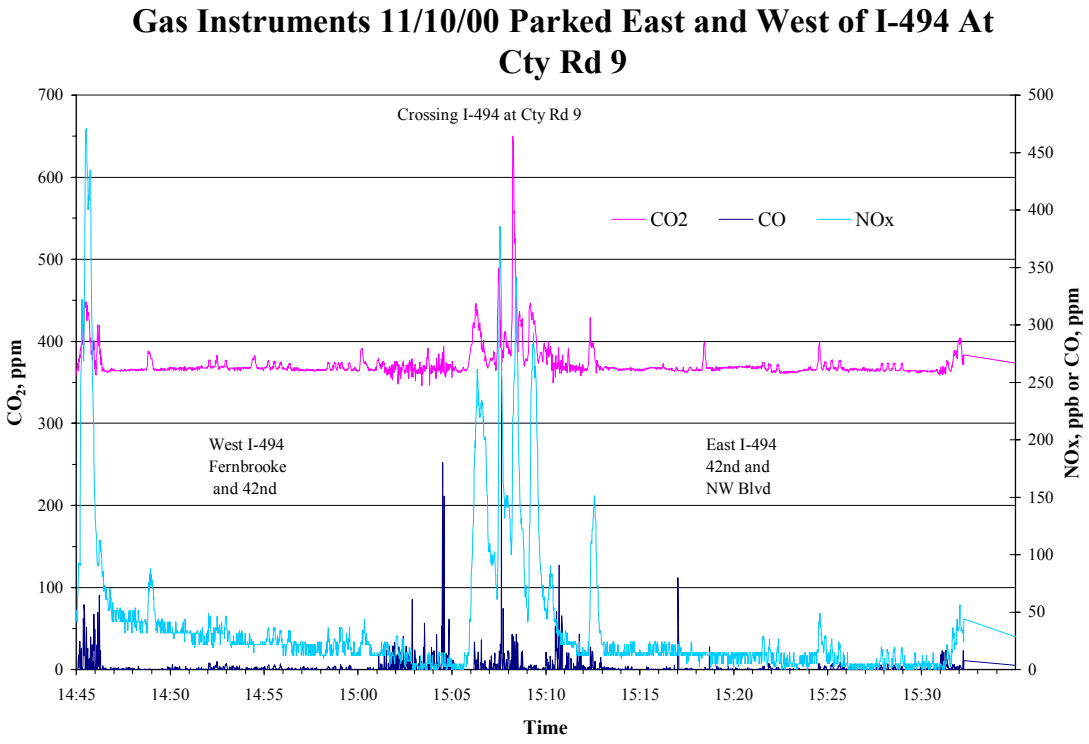

Figure 33. Gas Instruments 11/10/00 Parked East and West of I-494 At Cty Rd 9

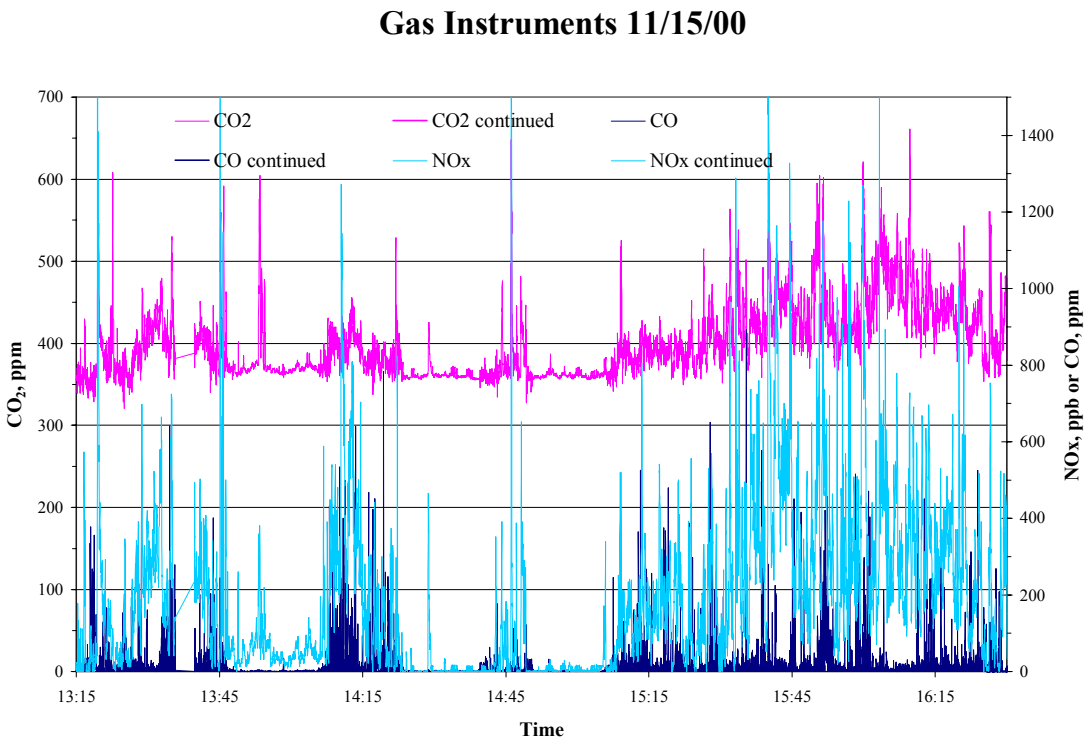

Figure 34. Gas Instruments 11/15/00

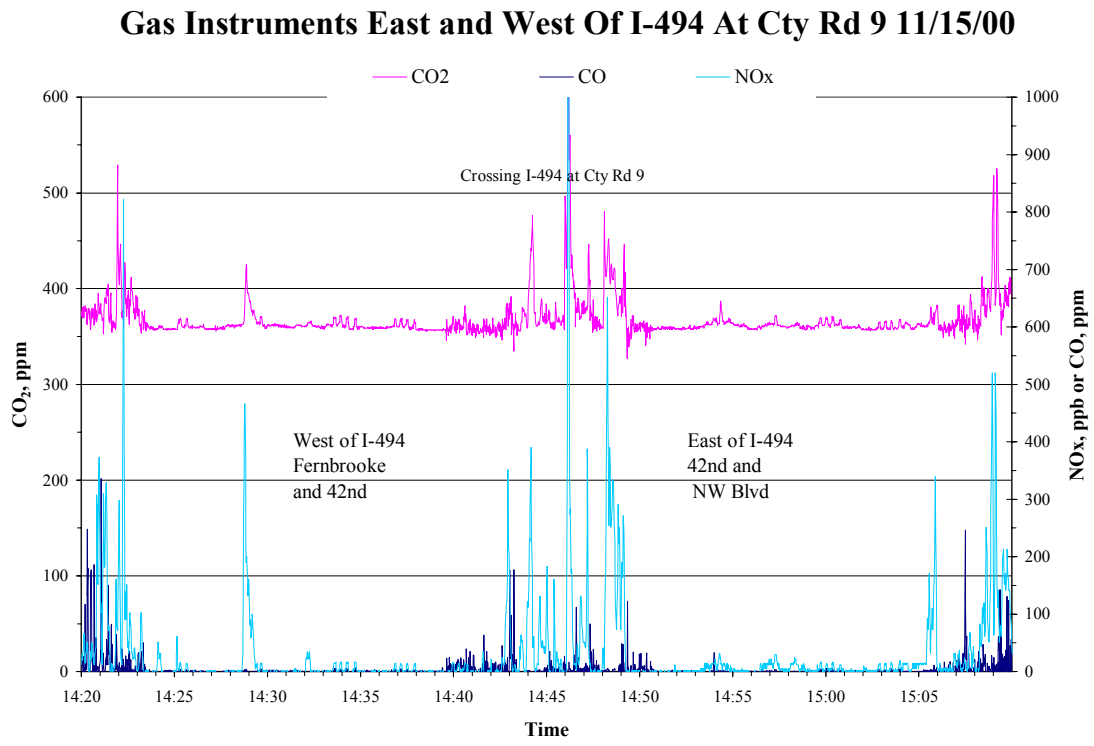

Figure 35. Gas Instruments East and West Of I-494 At Cty Rd 9 11/15/00

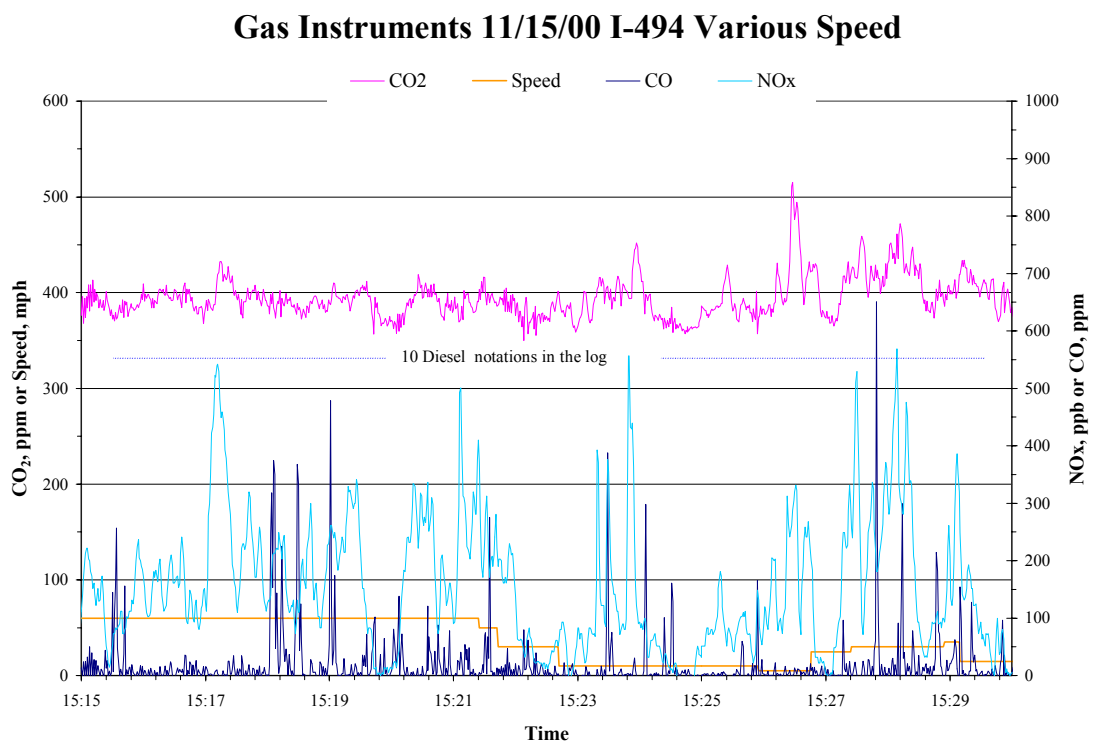

Figure 36. Gas Instruments 11/15/00 I-494 Various Speed

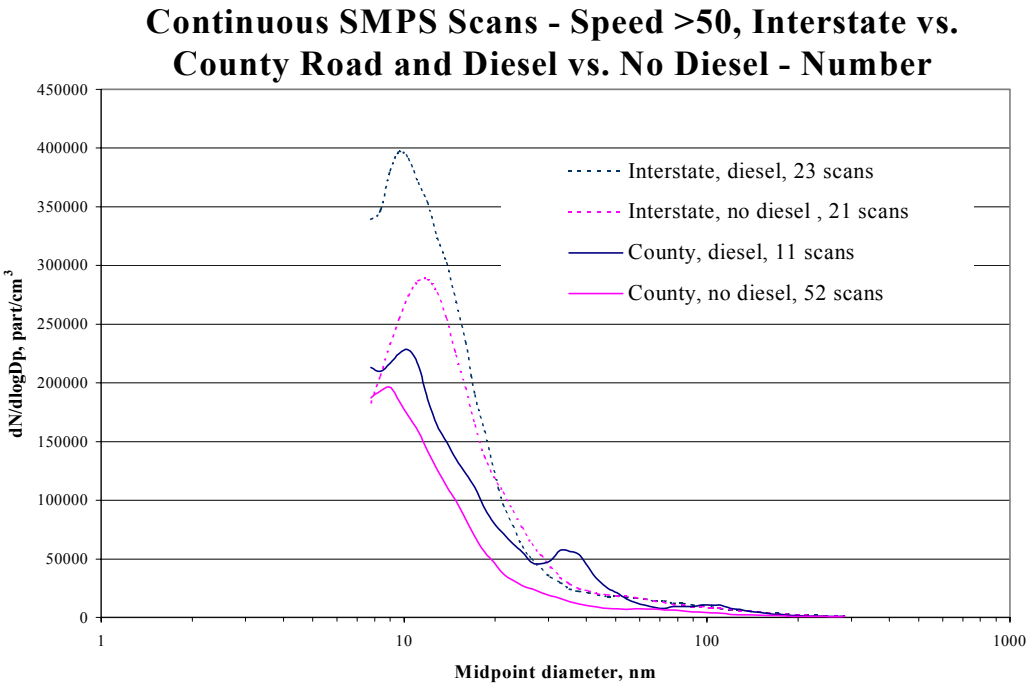

Figure 37. Continuous SMPS Scans – Speed > 50, Diesel vs. No Diesel – Number

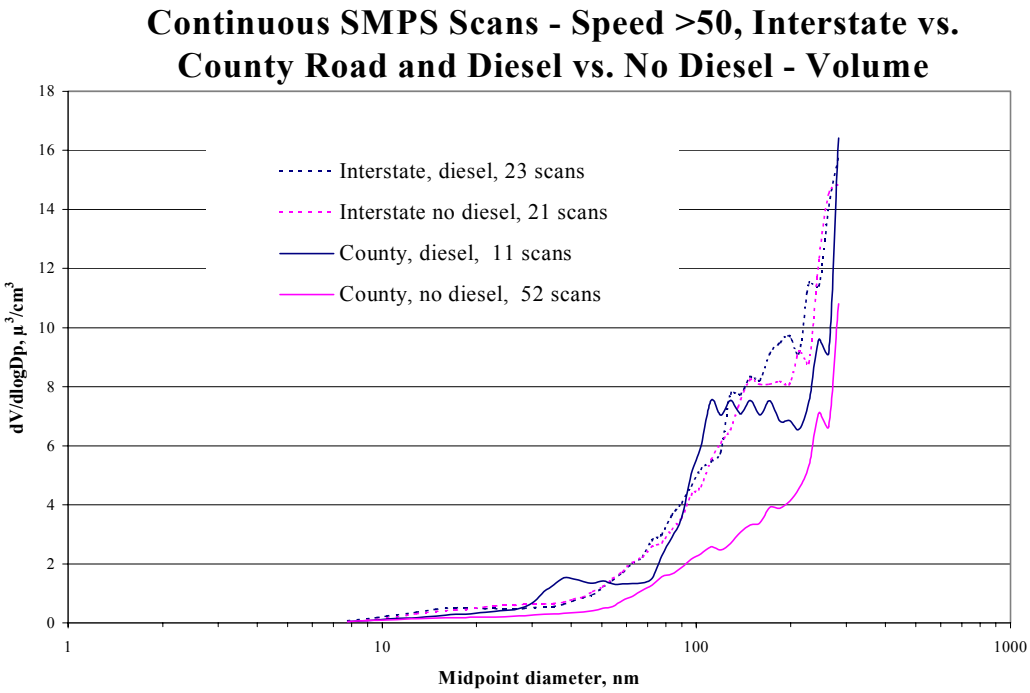

Figure 38. Continuous SMPS Scans – Speed > 50, Diesel vs. No Diesel – Volume

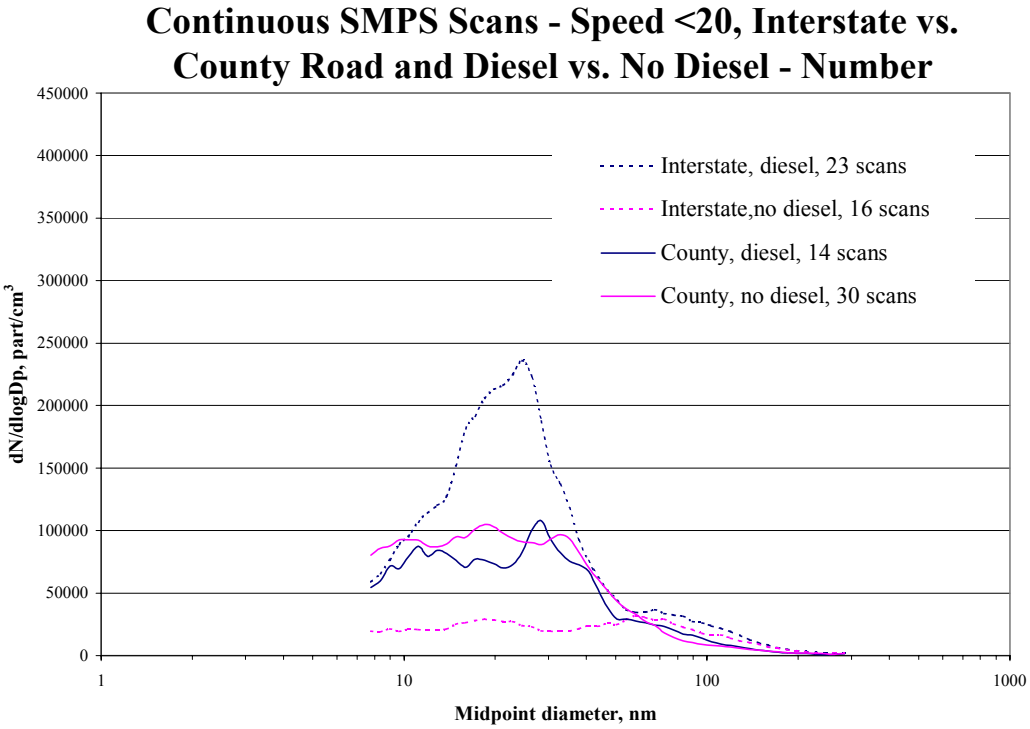

Figure 39. Continuous SMPS Scans – Speed < 20, Diesel vs. No Diesel – Number

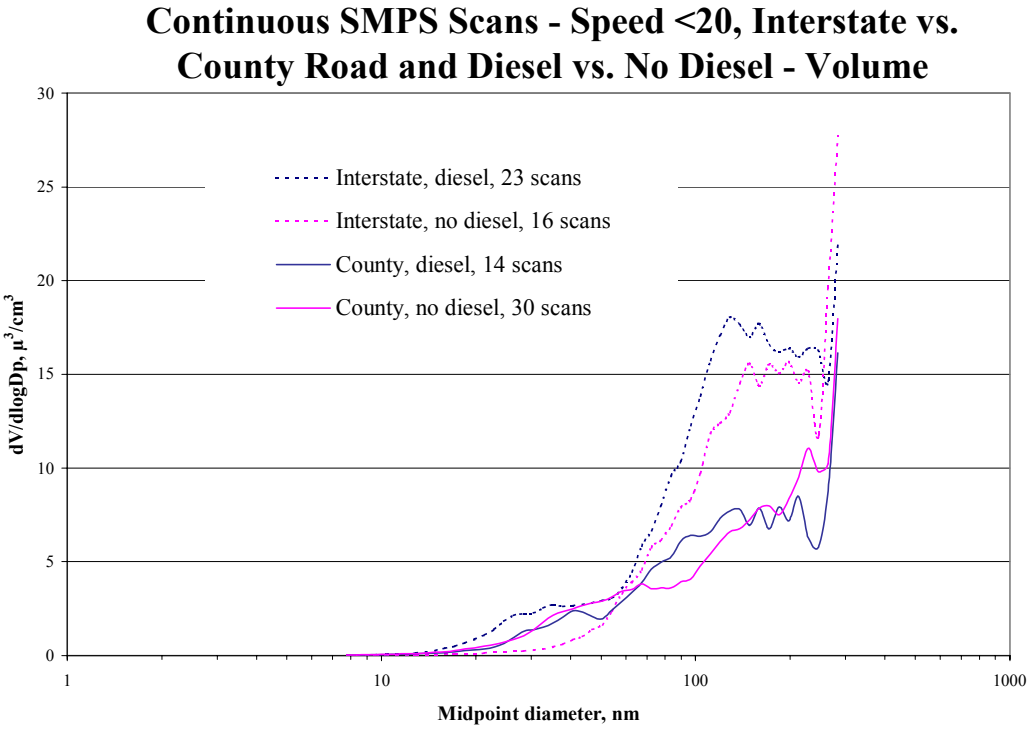

Figure 40. Continuous SMPS Scans – Speed < 20, Diesel vs. No Diesel – Volume

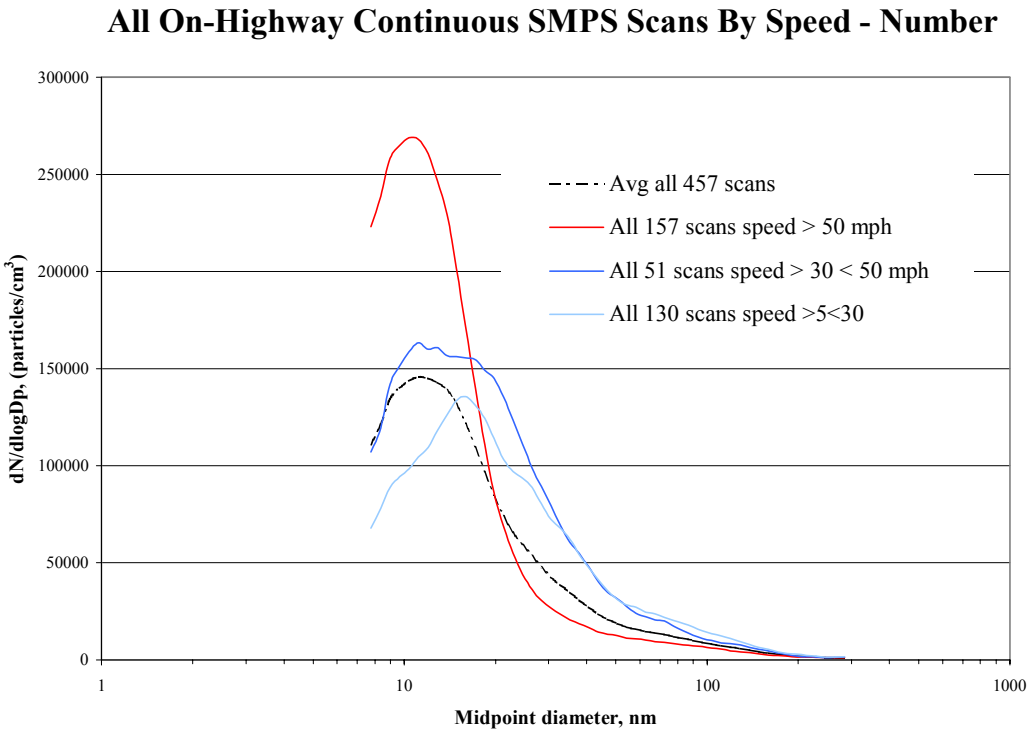

Figure 41. All On-Highway Continuous SMPS Scans By Speed – Number

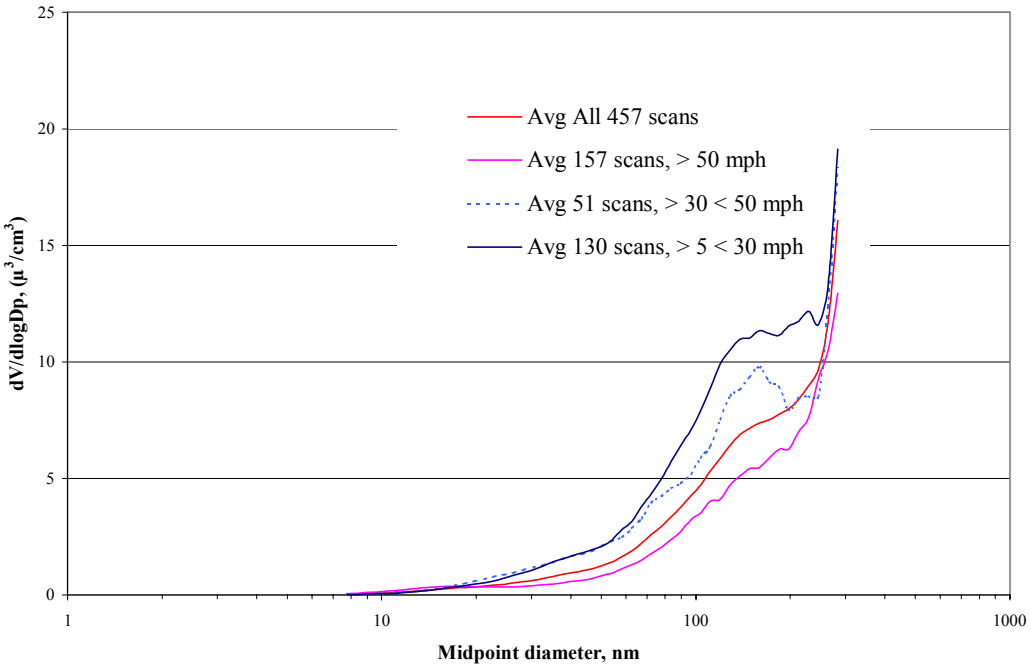

Figure 42. All On-Highway Continuous SMPS Scans By Speed – Volume

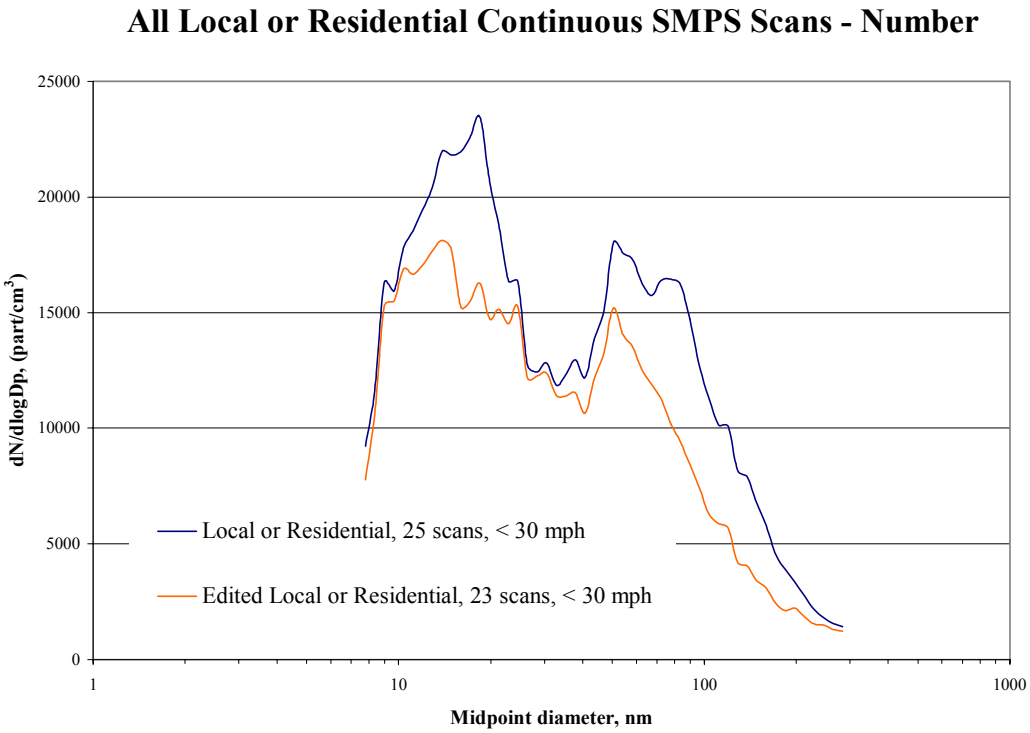

Figure 43. All Local or Residential Continuous SMPS Scans – Number

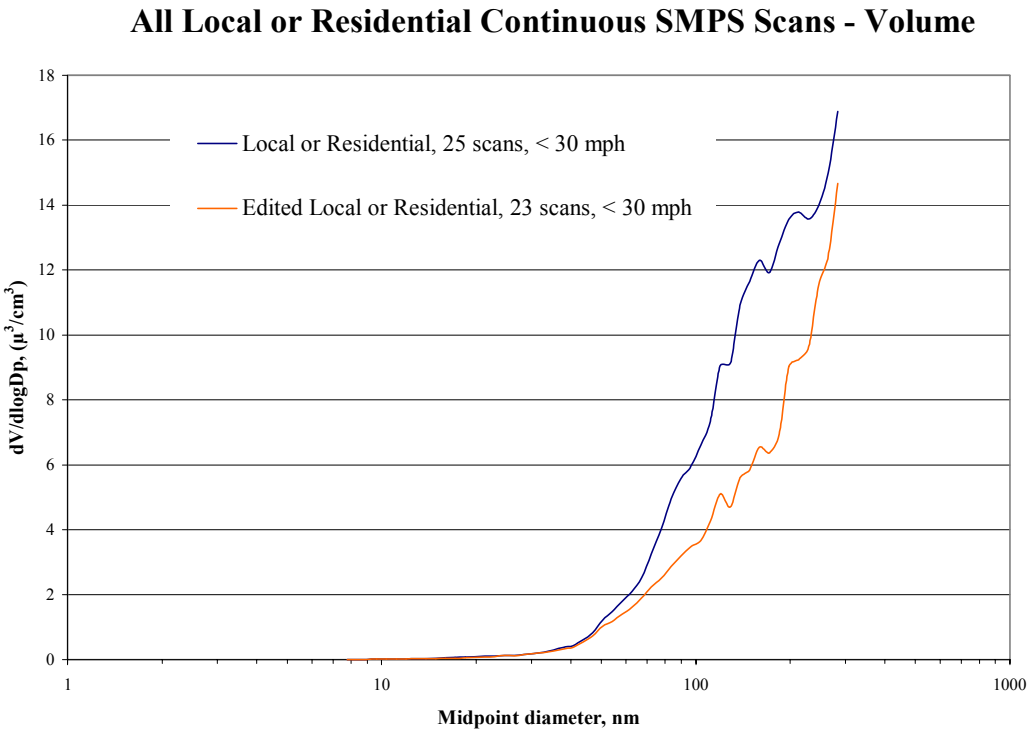

Figure 44. All Local or Residential Continuous SMPS Scans – Volume Distributions

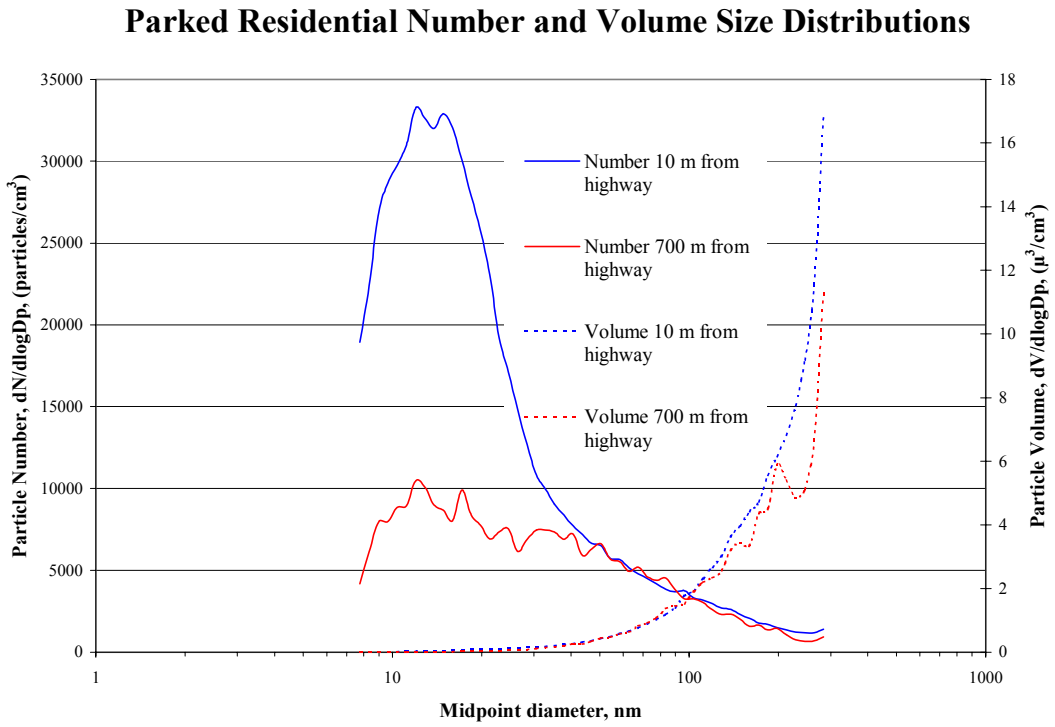

Figure 45. Parked Residential Number and Volume Size Distributions

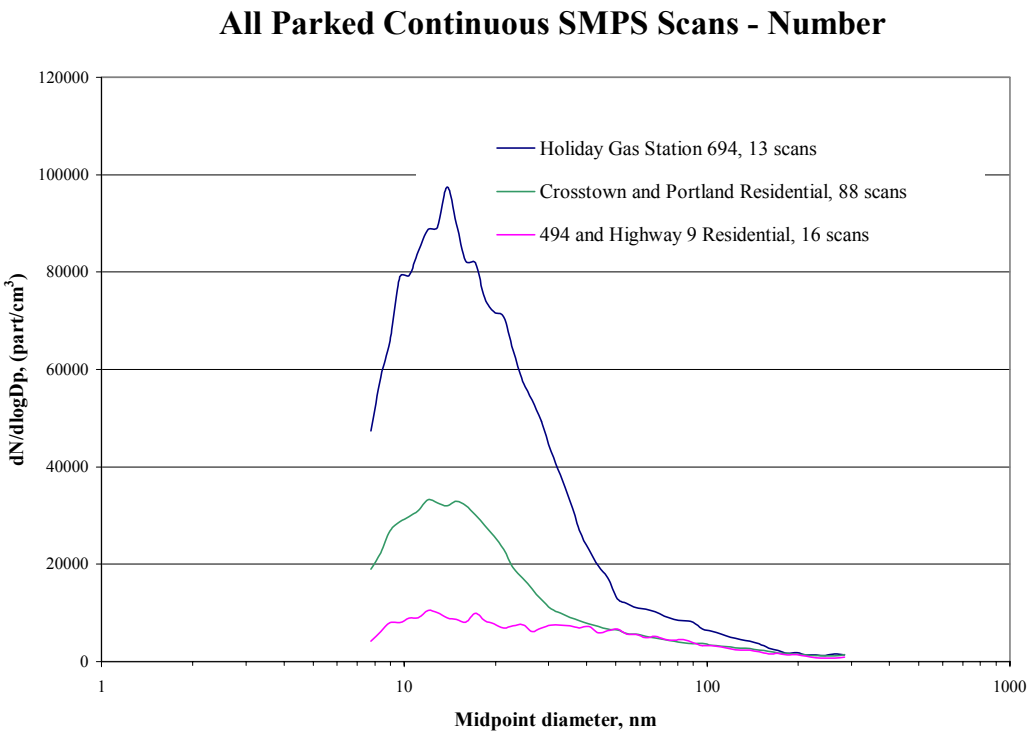

Figure 46. All Parked Continuous SMPS Scans – Number Distributions

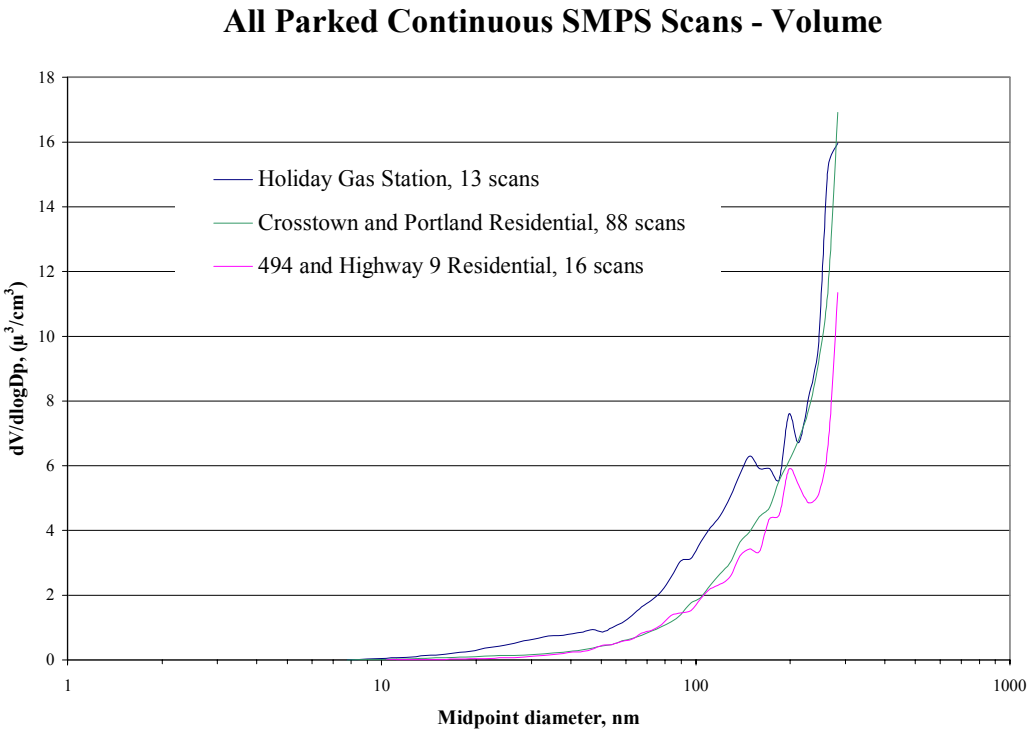

Figure 47. All Parked Continuous SMPS Scans – Volume Distributions

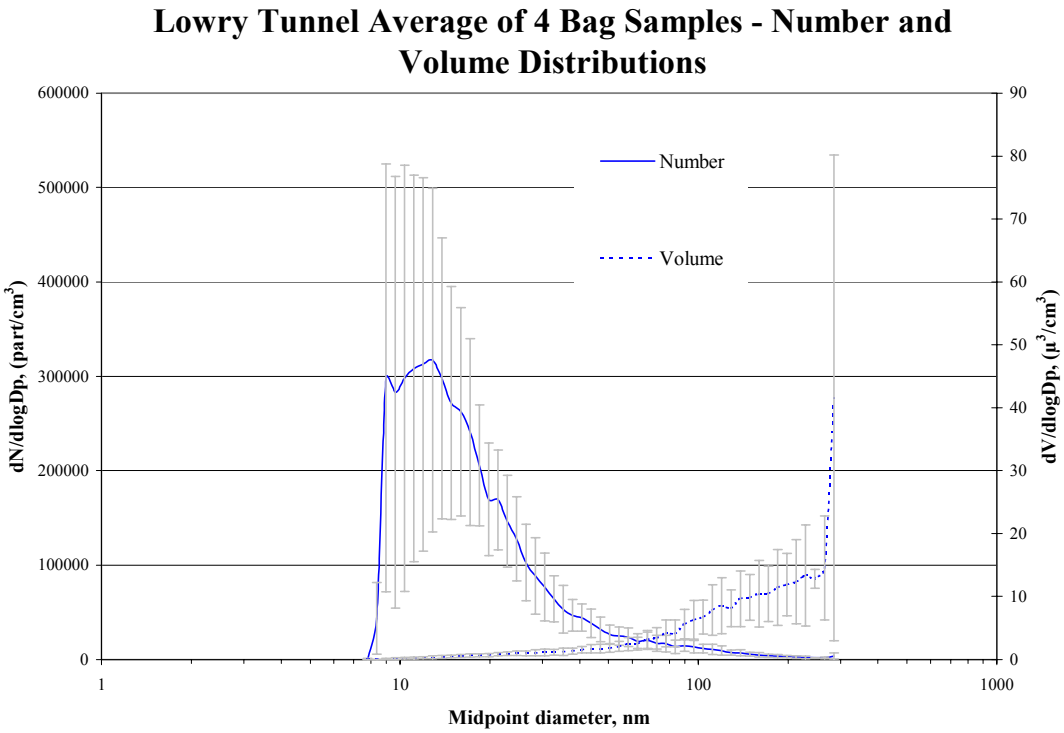

Figure 48. Lowry Tunnel Average of 4 Bag Samples – Number And Volume Distributions

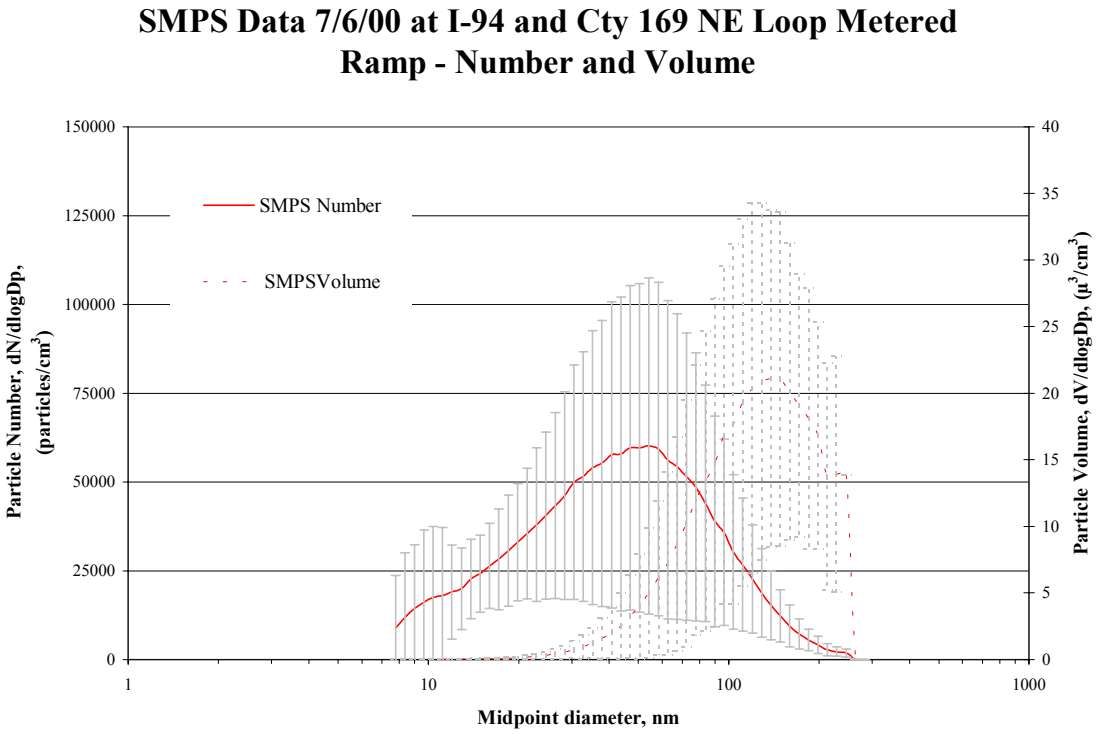

Figure 49. SMPS Data 7/6/00 At I-94 and Cty 169 NE Loop Metered Ramp

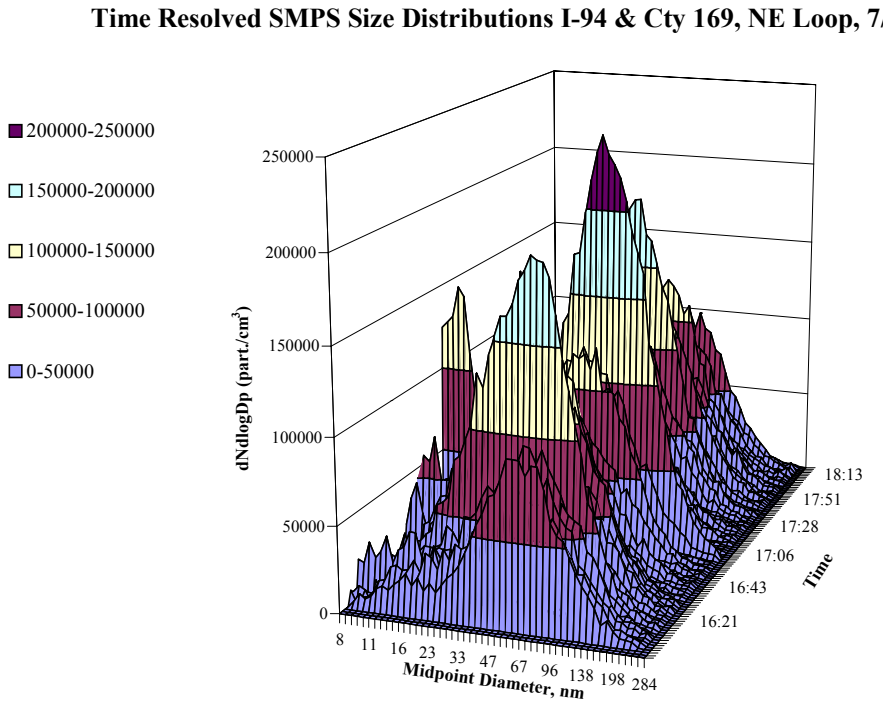

Figure 50. Time Resolved SMPS Size Distributions I-494 & Cty 169, NE Loop, 7/6/00

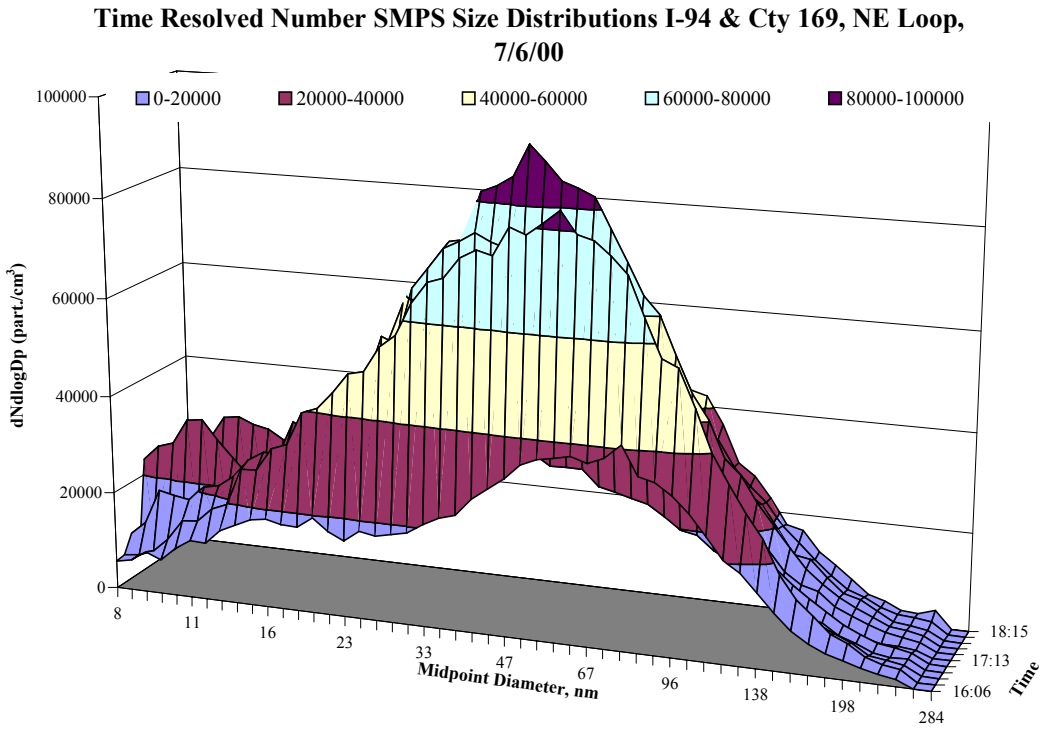

Figure 51. Number SMPS Size Distributions I-494 & Cty 169, NE Loop, 7/6/00

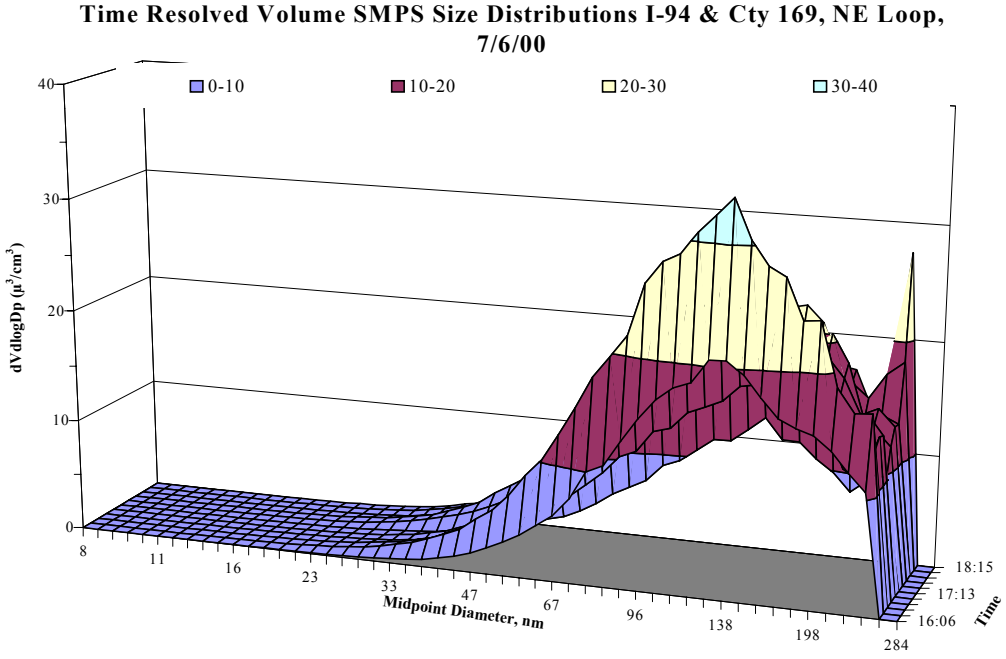

Figure 52. Volume SMPS Size Distributions I-494 & Cty 169, NE Loop, 7/6/00

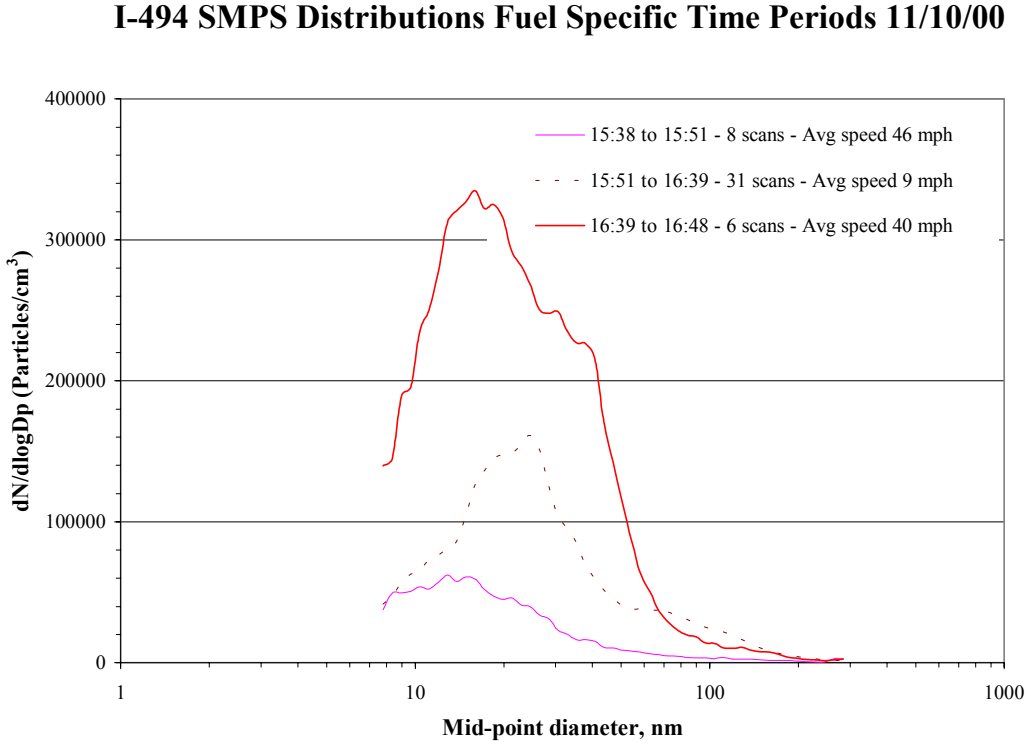

Figure 53. I-494 SMPS Distributions Fuel Specific Time Periods 11/10/00

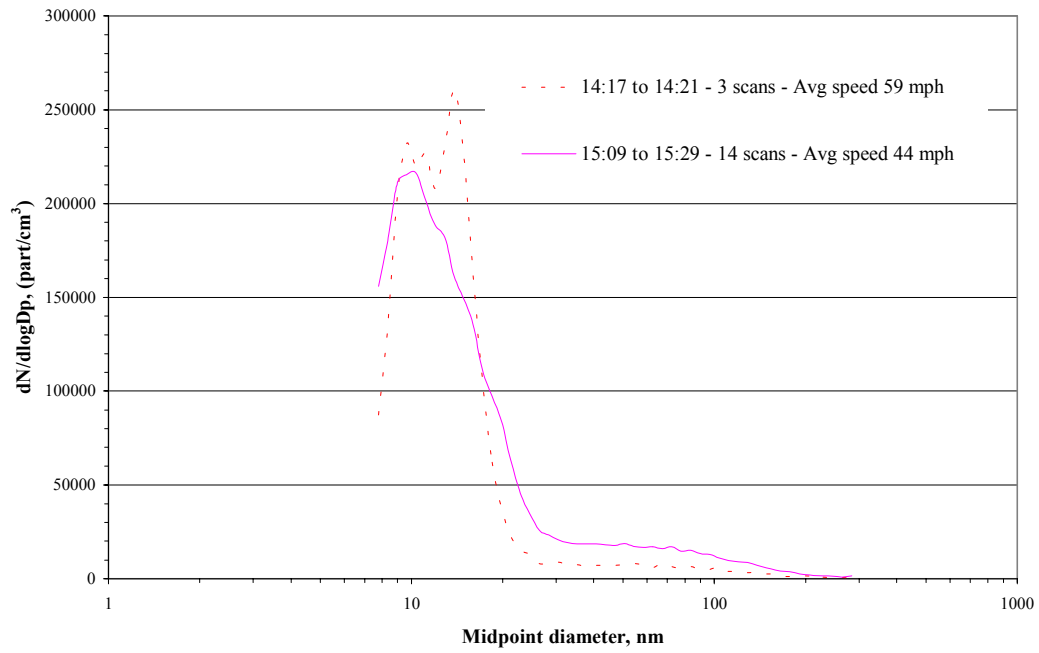

Figure 54. I-494 SMPS Distributions Fuel Specific Time Periods 11/15/00